JOINT INSTITUTE FOR NUCLEAR RESEARCH
Frank laboratory of Neutron physics

FINAL REPORT ON THE
SUMMER STUDENT PROGRAM

Optimization of Shielding-Collimator Parameters for ING-27 Neutron Generator, ROMASHA Setup, TANGRA Project using Artificial Neural Network (ANN).

Supervisor:
Dr. Vadim Skoy

Student:
Aya Hamdy, Faculty of Engineering Nuclear and Radiation Department, Alexandria University, Alexandria, Egypt.

Participation period:
July 02 – August 26
Dubna, 2017

Contents

Abstract

Neutron generators are now used in various fields. They produce only fast neutrons; the D-D neutron generator produces 2.45 MeV neutrons and the D-T neutron generator produces 14.1 MeV neutrons. In order to optimize shielding- collimator parameters to achieve higher neutron flux at the investigated sample with lower neutron and gamma rays flux at the area of the detector, design iterations are widely used, which consumes lots of time and computational power. The significance of this work is creating a generalized algorithm to optimize theses parameters using Artificial Neural Network (ANN).

The work was applied on ROMASHA setup, TANGRA project (TAgged Neutron and Gamma RAys) for studying neutron-induced nuclear reactions, Frank laboratory of neutron physics (FLNP), Joint institute for Nuclear Research (JINR).

The studied parameters were; (1) the shielding-collimator material; three materials were studied (2) Distance between shielding-collimator assembly first plate of ROMASHA setup and centre of the neutron beam, and (3) the thickness of collimator sheets; two thicknesses were studied for each plate.

MCNP5 was used to simulate ROMASHA setup after it was validated on the experimental results, MCNP5 results were extracted and used for training the classifiers and neural net fitting algorithms, then the results of the classifiers and neural net fitting algorithms were validated on MCNP5 results of the test cases.

Ratio between 14.1 MeV neutrons at the investigated sample and total neutron flux that enters each detector was calculated and plotted for all the studied parameters for each detector, concluding that the optimum shielding-collimator assembly is Tungsten of 5 cm thickness for each plate, and a distance of 2.3 cm.

And finally the ratio between 14.1 MeV neutrons at the investigated sample and total gamma rays flux that enters each detector from inelastic scattering of fast neutrons with the shielding material was calculated and plotted for all the studied parameters for each detector, leading to the previous conclusion but the distance was concluded to be 1 cm.

The main scope was to prove that neural networks can be used for solving the problem of optimization of the shielding-collimator parameters, saving time and computational power instead of the design iterations approach.

Introduction

The main advantage of neutron generators is its compact size. Neutron generators are now used in various fields and their applications are enormously increasing. They produce only fast neutrons; the D-D neutron generator produces 2.45 MeV neutrons and the D-T neutron generator produces 14.1 MeV neutrons. One of the problems of neutron generators is optimization of the parameters of neutron gamma shielding-collimator assembly [1]. The purpose of the optimization is to reach an acceptable value of the ratio between the neutron flux in the investigated sample (the signal) and the neutron flux in the area of the detectors (the background) as well as to reach as low as possible gamma rays from inelastic scattering of fast neutrons with shielding material.

In order to know the parameters of the of neutron gamma shielding-collimator assembly to achieve a specific neutron flux for irradiation of the sample with neutron energy of 14.1 MeV and to lower the neutron flux that enters the detectors, as well as lowering the gamma rays resulting from inelastic scattering of fast neutrons with the shielding assembly in comparison with gamma rays from the investigated sample, various simulations and experiments are needed for the design of the shielding-collimator assembly. The purpose of this work is to develop an algorithm that specifies the parameters of the shielding-collimator assembly for ING-27neutron generator using artificial neural network (ANN).

An Overview on the Artificial Neural Networks (ANNs)

The simplest definition of artificial neural network is provided by the inventor of one of the first neurocomputers, Dr. Robert Hecht Nielsen. He defines a neural network as:

"...a computing system made up of a number of simple, highly interconnected processing elements, which process information by their dynamic state response to external inputs. "

ANNs are processing devices (algorithms or actual hardware) that are loosely modeled after the neuronal structure of the mamalian cerebral cortex but on much smaller scales. A large ANN might have hundreds or thousands of processor units, whereas a mamalian brain has billions of neurons with a corresponding increase in magnitude of their overall interaction and emergent behavior.

Neural networks are typically organized in layers made up of a number of interconnected 'nodes' which contain an 'activation function'. Patterns are presented to the network via the ' input layer ', the answer is presented through the ' output layer '. Processing is done via a system of weighted connections ' hidden layers' which links the input to the output. As shown in figure 1.

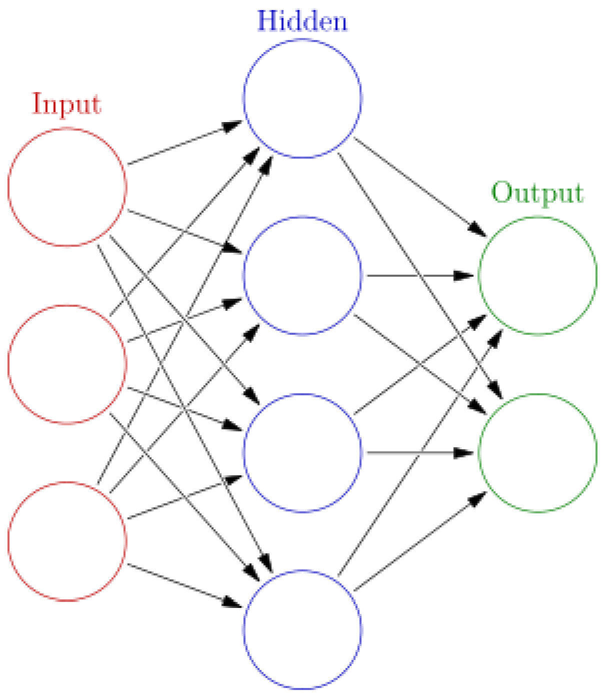

Figure 1. Neural Network Diagram.

Most ANNs contain some form of 'learning rule' which modifies the weights of the connections according to the input patterns. In a sense, ANNs learn by example as do their biological counterparts; a child learns how to recognize things by examples.

Although there are many different kinds of learning rules used by neural networks, this work is concerned only with one; the delta rule. The delta rule is often utilized by the most common class of ANNs called 'backpropagational neural networks' (BPNNs). Backpropagation is an abbreviation for the backwards propagation of error.

With the delta rule, as with other types of backpropagation, 'learning' is a supervised process that occurs with each cycle or 'epoch' (i.e. each time the network is presented with a new input pattern) through a forward activation flow of outputs, and the backwards error propagation of weight adjustments. More simply, when a neural network is initially presented with a pattern it makes a random 'guess' as to what it might be and then sees how far its answer was from the actual one and makes an appropriate adjustment to its connection weights. [2]

Data preprocessing

Principle component analysis (PCA)

One of the difficulties inherent in multivariate statistics is the problem of visualizing data that has many variables. Fortunately, in data sets with many variables, groups of variables often move together. One reason for this is that more than one variable might be measuring the same driving principle governing the behavior of the system. In many systems there are only a few such driving forces. When this happens, you can take advantage of this redundancy of information. You can simplify the problem by replacing a group of variables with a single new variable. Principal component analysis is a quantitatively rigorous method for achieving this simplification. The method generates a new set of variables, called principal components. Each principal component is a linear combination of the original variables. All the principal components are orthogonal to each other, so there is no redundant information. The principal components as a whole form an orthogonal basis for the space of the data. The first principal component is a single axis in space. When you project each observation on that axis, the resulting values form a new variable. And the variance of this variable is the maximum among all possible choices of the first axis.

The second principal component is another axis in space, perpendicular to the first. Projecting the observations on this axis generates another new variable. The variance of this variable is the maximum among all possible choices of this second axis. [3]

Literature Survey

E.S.Konobeevsky et al, have optimized the collimator and shielding of the NG 430 neutron generator at the Institute for Nuclear Research, Russian Academy of Sciences. The purpose of the work was to achieve an acceptable ratio between the useful signal and the background; below, this ratio is denoted by *Q.*

The parameters for optimizing the *Q* value are the collimator thickness along the neutron beam axis and the shielding thickness around the detectors, collimator, and DT neutron source. The experiment was modeled by the Monte Carlo method using the MCNP5 and SHIELD transport codes.

Various simulations and steps have been done. In the first stage of modeling, only the collimator's thickness *L* along the neutron beam axis was varied: *L* = 74, 108, 144, 180, 216 cm.

In the second stage of modeling, a shielding layer of borated polyethylene with a thickness of 20 cm was introduced around the collimator and the detecting area in order to increase the *Q* values.

In the final stage of modeling, the possibility of further increasing the *Q* values was studied and investigated the dependence of *Q* on the thickness of the shielding layer around the collimator and detectors. [4]

D.L. Chichester et al, have optimized the biological shield for D-T neutron generator. The modeling used in these simulations was performed using the MCNP 4C Monte Carlo code to investigate neutron and photon dose rates resulting from a 14.1 MeV point-like isotropic DT neutron source. [5]

Bergaoui et al. have optimized a neutron radiography system for non-destructive testing that uses 2.45 MeV D-D neutron generator. Various divergent truncated conic collimators were modeled using Monte Carlo N-Particle Transport Code (MCNPX 2.7.0). [6]

Significance

Literature has shown that design iterations are widely used for the determination of shielding- collimator parameters for each certain application, which consumes lots of time and computational power. The significance of this work is creating a generalized algorithm to optimize theses parameters using Artificial Neural Network (ANN).

The work was applied on the experimental setup TANGRA (TAgged Neutron and Gamma RAys) for studying neutron-induced nuclear reactions, Frank laboratory of neutron physics (FLNP), Joint institute for Nuclear Research (JINR). [7]

The algorithm will be able to predict the shielding-collimator parameters based on 14.1 MeV neutron flux that reaches the investigated sample in addition to the total neutron and gamma rays fluxes in the area of the detectors.

The studied parameters were; (1) the shielding-collimator material; three materials were studied: Iron, Tungsten, Tungsten alloy (90% Tungsten, 7% Nickel, and 3% Iron), (2) Distance between the shielding-collimator assembly first plate of ROMASHA setup (will be described in details later) and centre of the neutron beam, while the other distances were set to be functions of the studied distance, and (3) the thickness of shielding-collimator sheets; two thicknesses for each plate were studied 4 cm and 5 cm.

TANGRA setup

The TANGRA-setup consists of a portable neutron generator (ING-27) for producing a continuous beam of 14.1 MeV neutrons, a compact neutron-gamma shielding-collimator assembly and an array of 22 hexagonal NaI (Tl), 10 BGO cylindrical detectors for gamma-ray and neutron spectroscopy in variable configurations. The current configuration utilizes 10 cylindrical BGO gamma-ray detectors (ROMASHA setup), figure 3. While the previous configuration was 22 hexagonal NaI (TI) gamma-ray detectors (ROMASHKA setup) [8], [9], figure 2. A 32 channel multi-parametric digital data acquisition system (DAQ) is used for analog signal processing.

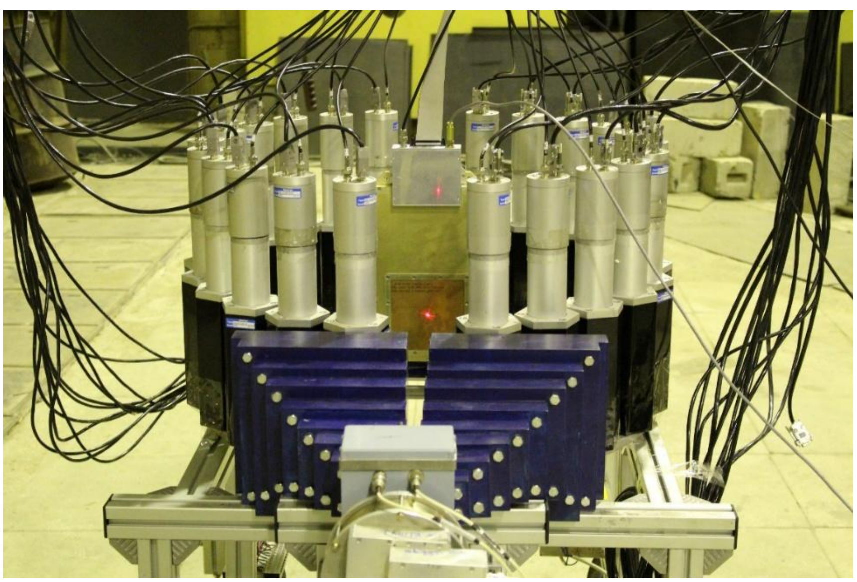

Figure 2. ROMASHKA setup, 22 hexagonal NaI (TI) gamma-ray detectors.

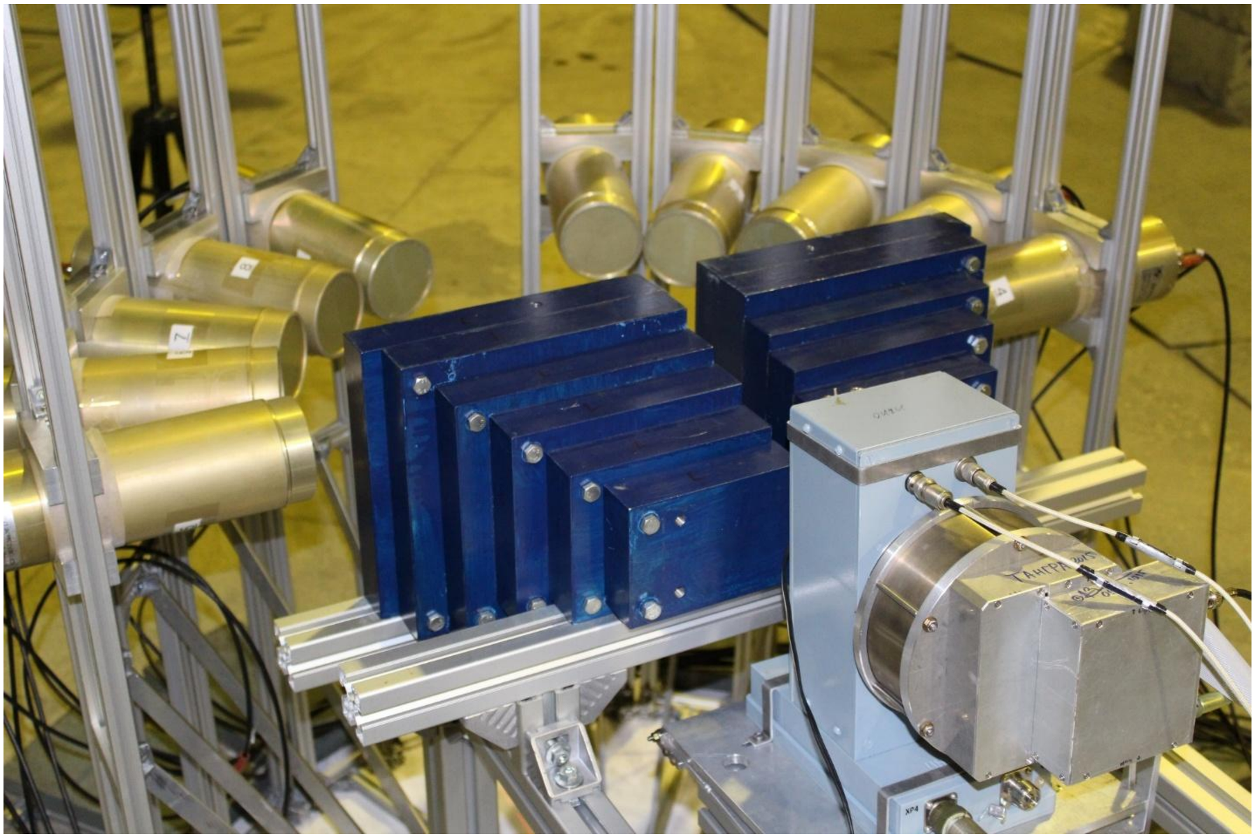

Figure 3. ROMASHA setup, 10 BGO (Bi4Ge3O12) detectors.

ING-27 neutron generator

ING-27 D-T neutron generator is a small-size generator of new generation based on sealed gas-filled neutron tube with a built-in multi-pixel alpha particles detector.

New equipment for remote detection and identification of explosive and other hazardous materials using associated particle imaging method (API) is designed on the basis of ING-27. The generator is designed to operate in computer-based hardware systems, both stationary and mobile, Consists of neutron emission unit with alpha detector, power supply and control unit, connection cables up to 15 m long. It was produced by N.L. Dukhov All Russia Research Institute of Automatics (VNIIA), technical characteristics are shown in table 1. [10]

Table. 1 Technical Characteristics of the ING-27 Neutron Generator	
Neutron energy, MeV	14.1
Neutron flux, n/s	Up to 10^8
Alpha detector emission mode	Continuous
Number of alpha detector pixels	64
Power supply, V	+200
Maximum power consumption, W	40
Operating lifetime, h (at neutron flux of 5 $\times 10^7$ neutron/s)	1000

Dimensions, mm: **- neutron emission unit** **- power supply and control unit**	220×130×179 279×193×94
Weight, kg: **- neutron emission unit** **- power supply and control unit**	 7.0 3.0

The current configuration of shielding-collimator assembly consists of 6 plates each one is 4 cm thick and made of iron as shown in figure 4. The distance between each plate and centre of the Neutron beam is approximately 2, 2.1, 2.25, 2.45, 2.6, 2.7 Cm.

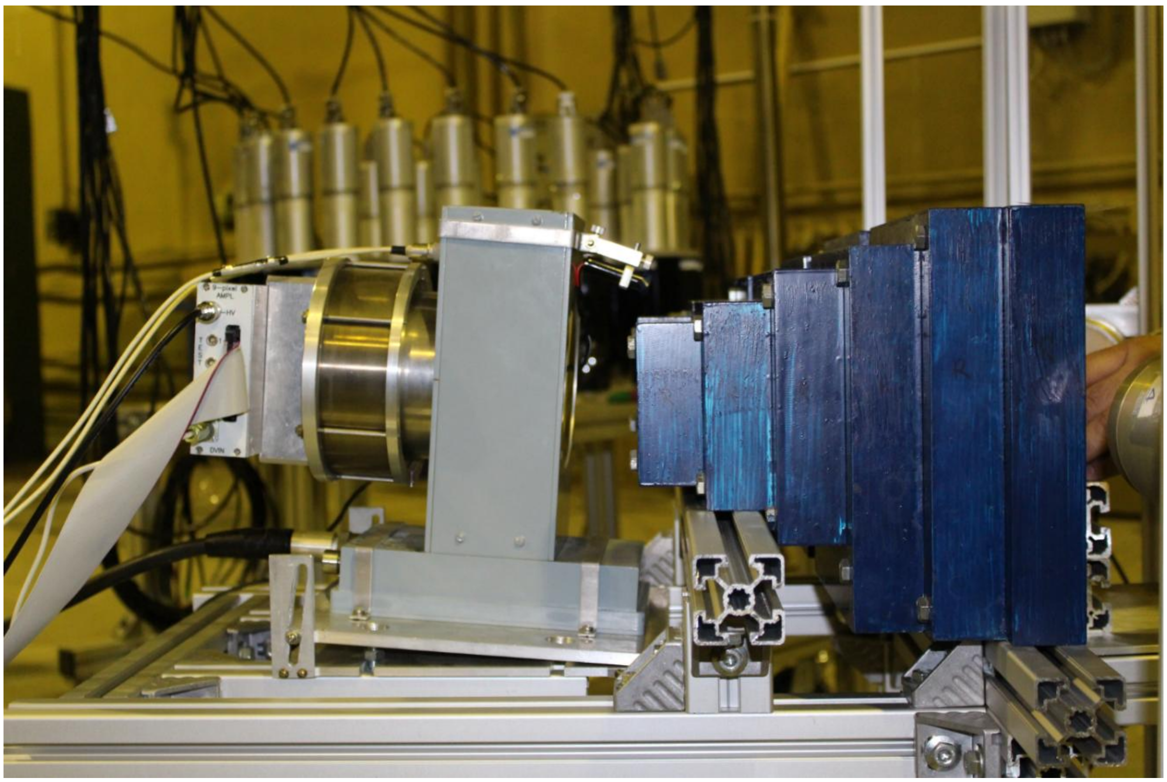

Figure 4. Neutron generator ING-27 and the iron shielding-collimator.

Methodology

MCNP5 model was developed for the ROMASHA setup assuming the neutron source to be a point source and the 10 BGO detectors to be cylinders placed at the specified locations in space as shown in figure 5. The experiment upon which the model was validated was the irradiation of a parallelepiped Carbon-12 sample for one hour to detect the 4.44 MeV characteristic gamma line of Carbon-12. The 4.44 MeV peak output from the MCNP5 was fitted to a Gaussian distribution and compared to the experimental output of the 10 detectors (channels), peak energy counts for both experimental results and MCNP5 results were compared and the full width half maximum as well as the resolution were calculated for each detector as shown in table 2. Figures 6.a - 6.j show the experimental results and MCNP5 results, where the smooth orange curve represents the MCNP5 results and the sharp blue curve represents the experimental results.

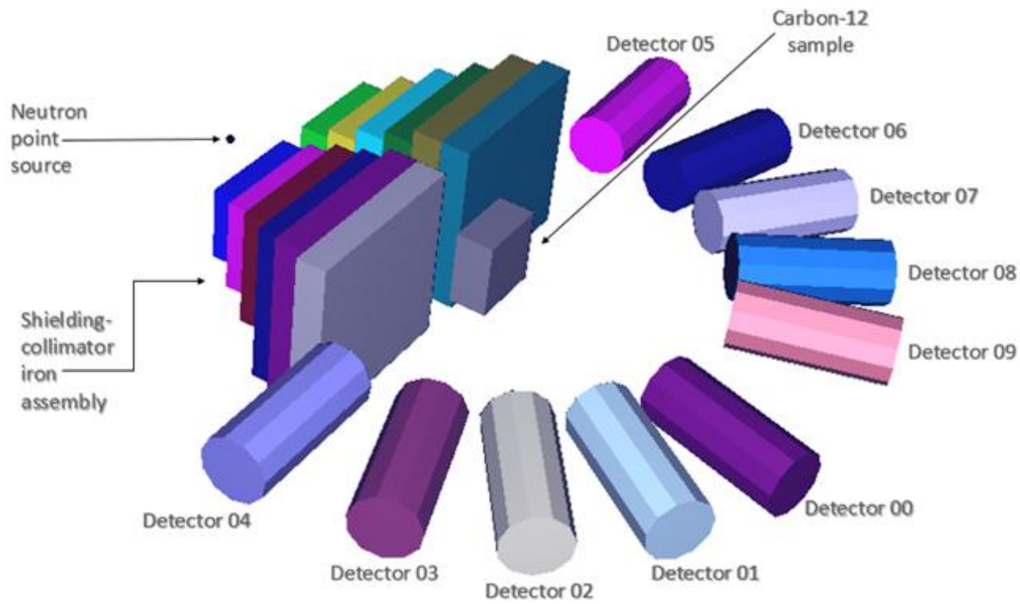

Figure 5. ROMASHA Setup MCNP5 Model

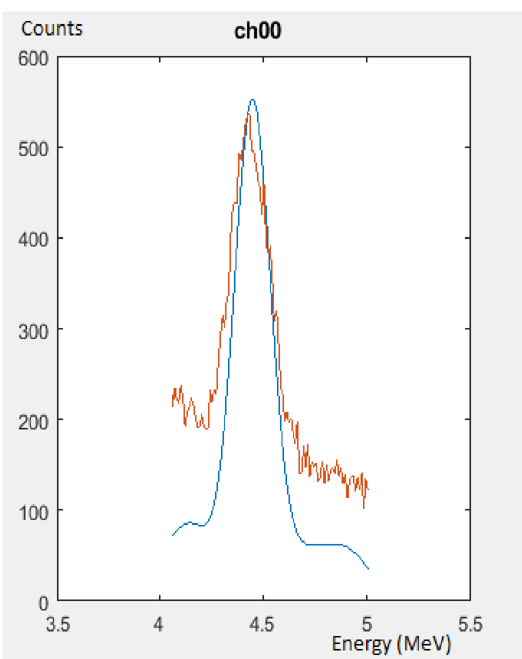

Figure 6.a. Validation of MCNP results on experimental results for detector 00.

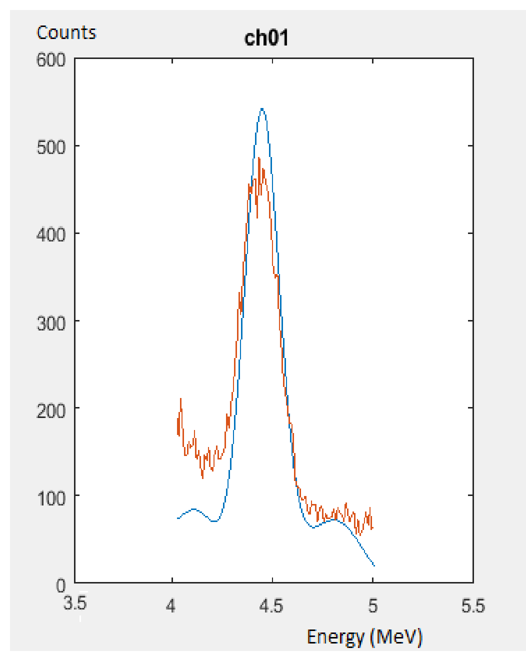

Figure 6.b. Validation of MCNP results on experimental results for detector 01.

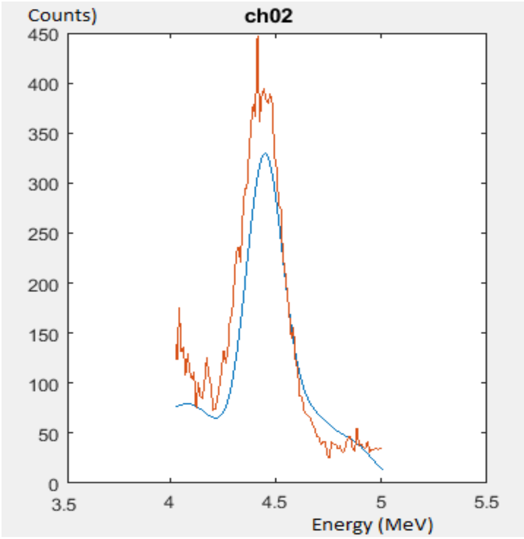

Figure 6.c.Validation of MCNP results on experimental results for detector 02.

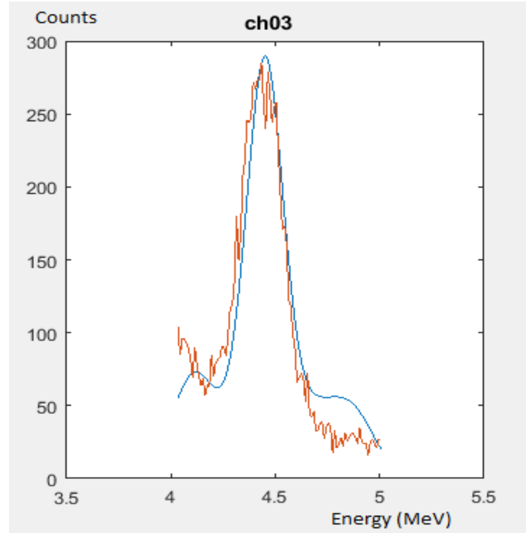

Figure 6.d. Validation of MCNP results on experimental results for detector 03.

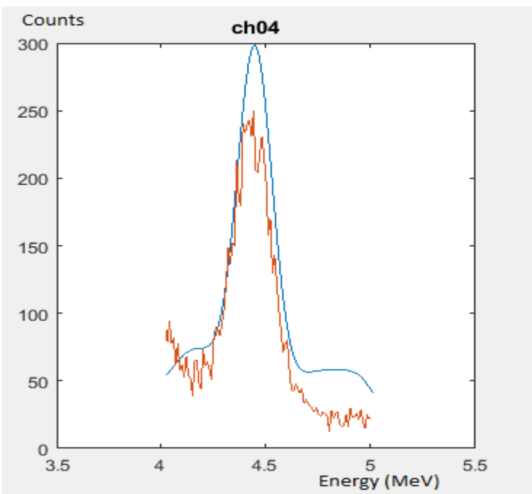

Figure 6.e. Validation of MCNP results on experimental results for detector 04.

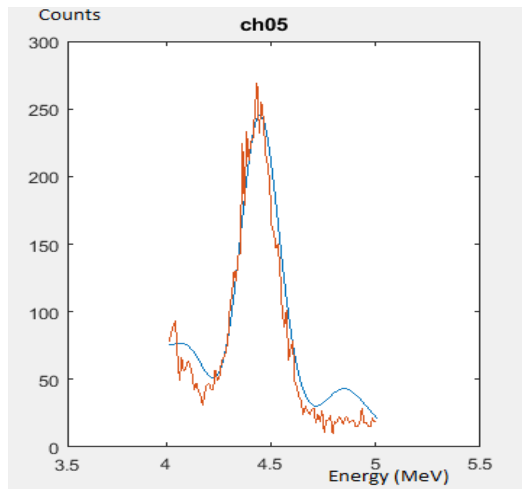

Figure 6.f. Validation of MCNP results on experimental results for detector 05.

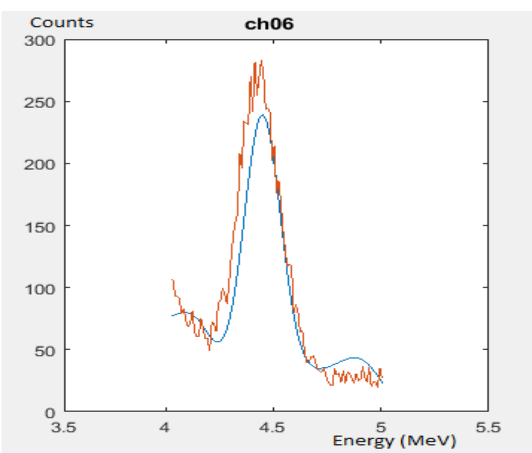

Figure 6.g. Validation of MCNP results on experimental results for detector 06.

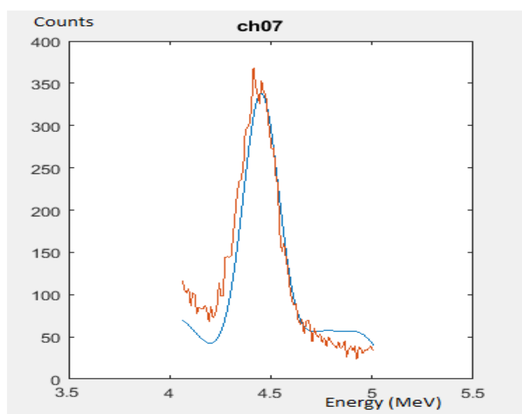

Figure 6.h. Validation of MCNP results on experimental results for detector 07.

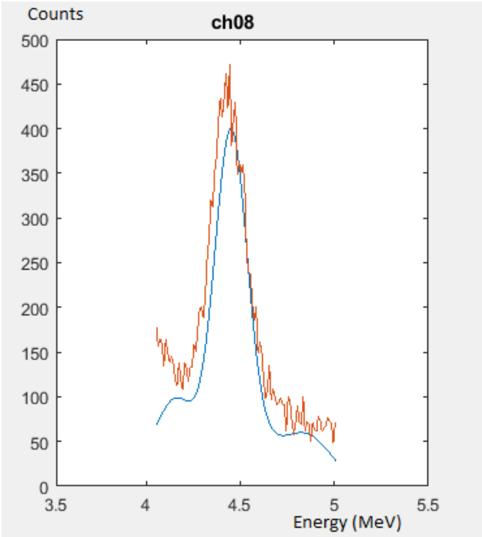

Figure 6.i. Validation of MCNP results on experimental results for detector 08.

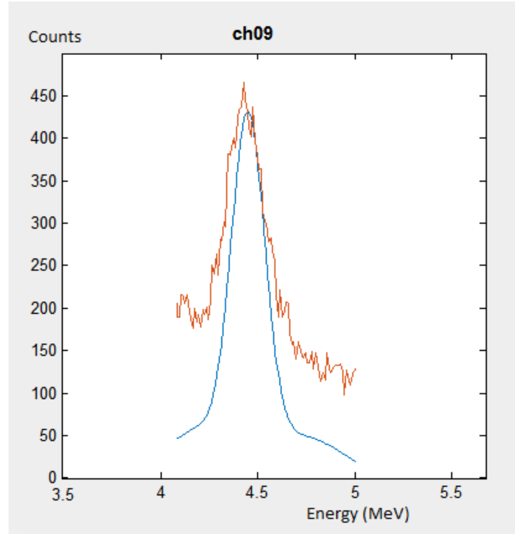

Figure 6.j. Validation of MCNP results on experimental results for detector 09.

Table 2. Validation Results of the MCNP5 Model

Detector number	Peak counts of experimental results	Peak counts of MCNP5 results	Difference between experimental and MCNP5 peak counts	FWHM (MeV)	Resolution (%)
00	537	548.208	11.208	0.29	6.54
01	486	527.32	41.32	0.24	5.41
02	387	329.095	57.905	0.25	5.64
03	285	287.769	2.769	0.235	5.29
04	250	298.685	48.685	0.25	5.64
05	232	245.2388	13.2388	0.2	4.51
06	270	237.2255	32.7745	0.245	5.52
07	338	334.69	3.31	0.23	5.18
08	423	404.186	18.814	0.245	5.52
09	431	420.66	10.34	0.335	7.55

After the validation process, the methodology adopted consisted of several steps shown in figure 7; (1) Data generation and extraction from the validated MCNP5 model after removing the sample for the training of the classifiers and the fitting neural network, (2) the classifier which differentiates between the different proposed shielding-collimator materials is trained, (3) the three classifiers that differentiate between the two thicknesses of the shielding-collimator plates for each material is then trained, and (4) for each thickness and material there was a fitting neural network designed for evaluating the distance between the first plate and center of the neutron beam. Distance for training was varied from 0.1 to 5.6 cm with step of 0.1 cm while the distance for test cases was varied from 0.15 to 5.65 with step of 0.1 cm.

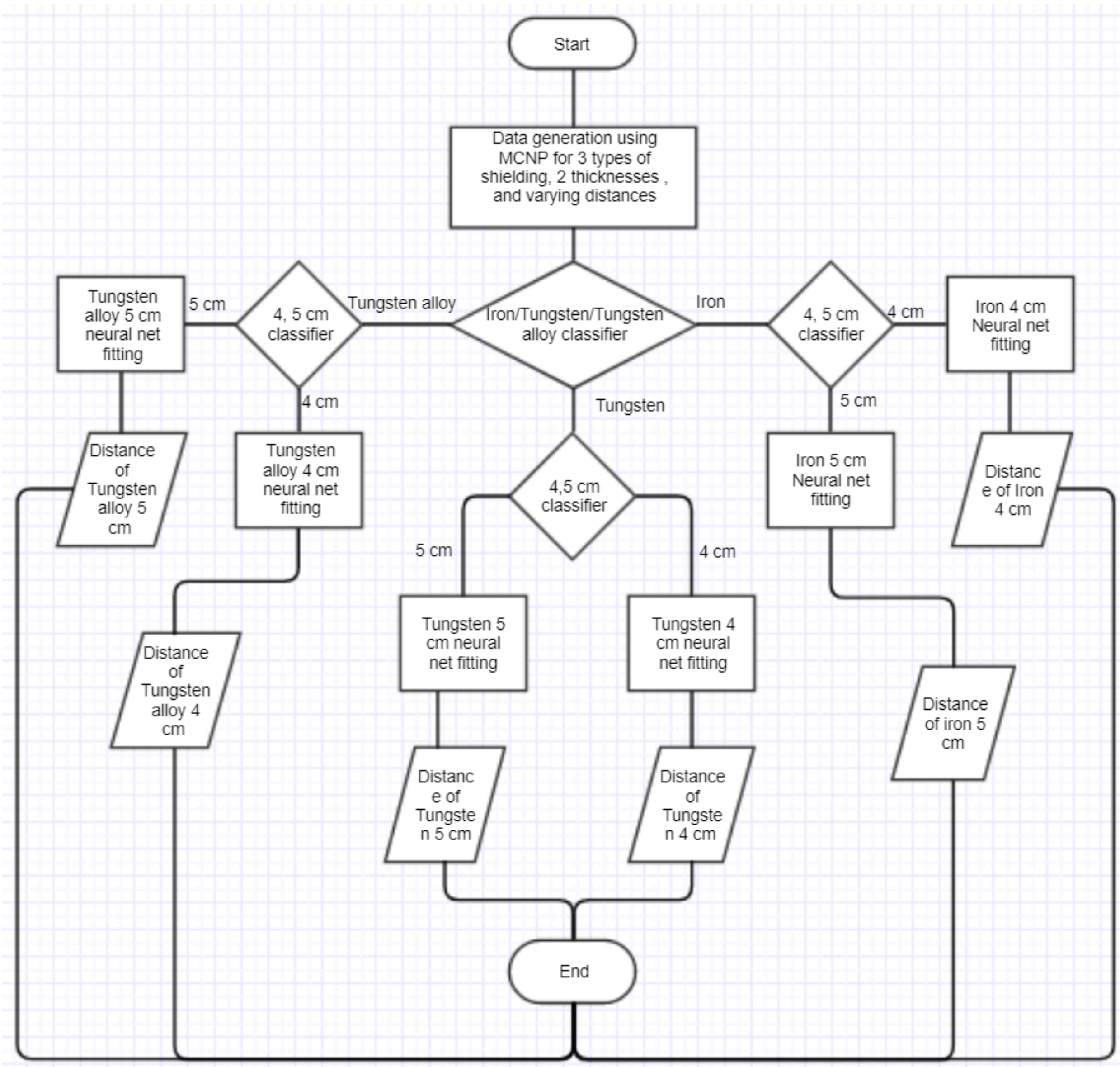

Figure 7. Flowchart of the methodology.

Results and Discussion

Neural Network Model Validation

The first classifier which differentiates between three types of materials (Iron, Tungsten, and Tungsten Alloy) discussed for the shielding-collimator sheets has shown training accuracy of 98.2% as shown in the confusion matrix shown in figure 8 where 1 denotes the iron shielding- collimator assembly, 2 denotes the tungsten shielding- collimator assembly, and 3 denotes the tungsten alloy. Also, the classifier has shown validation accuracy of 99.4% based on 336 test cases. The other three classifiers which classify for each material the thickness of its shielding-collimator sheets whether it is 4 or 5 cm has shown training accuracy of 100% and validation accuracy of 100% based on 112 test cases for each one of them as shown in the ROC figures 9.a, 9.b, and 9.c . The six developed fitting neural networks regression and validation are shown in figures 10.a - 10.f, and 11.a – 11.f respectively. The regression curves in the mentioned figures has shown almost 100% accuracy, while the validation curves has shown that the model results is almost identical to the real distances, mean absolute error (MAE) and standard error for each curve were calculated and shown in table 3.

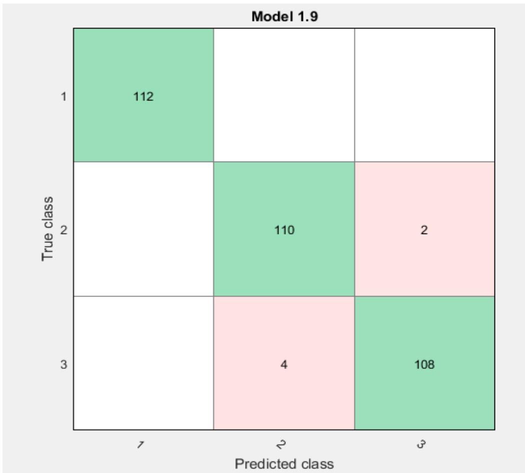

Figure8. Confusion matrix of materials classifier.

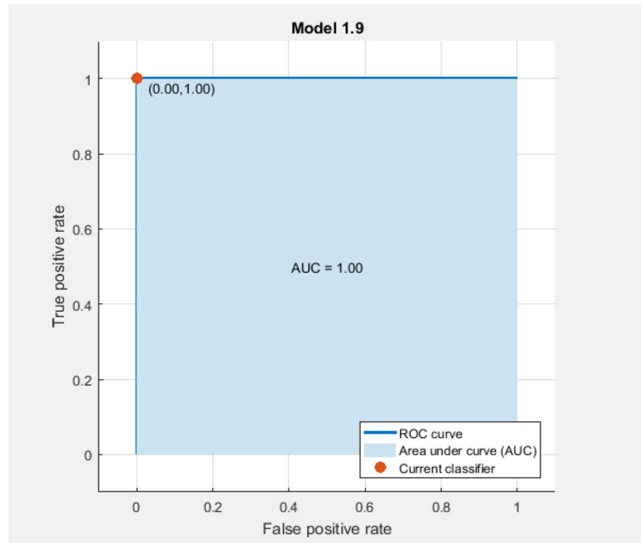

Figure 9.a. ROC curve of thickness classifier for iron shield.

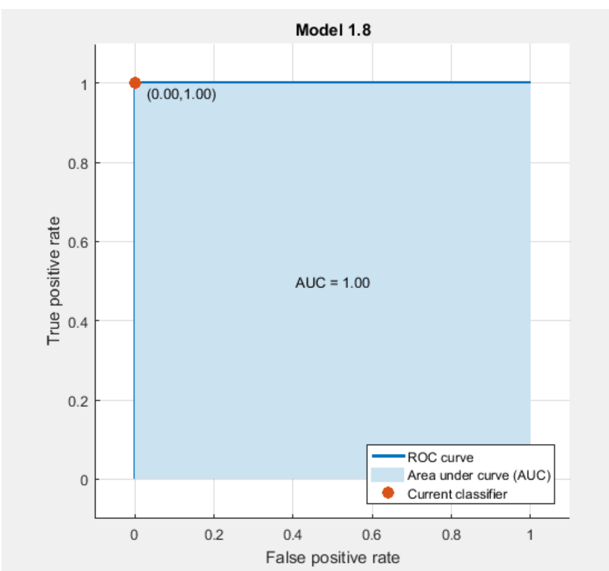

Figure 9.b. ROC curve of thickness classifier for Tungsten shield.

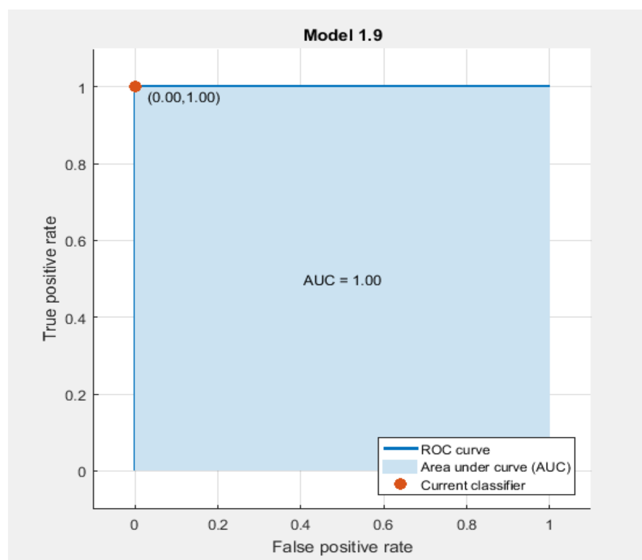

Figure 9.c. ROC curve of thickness classifier for Tungsten alloy shield.

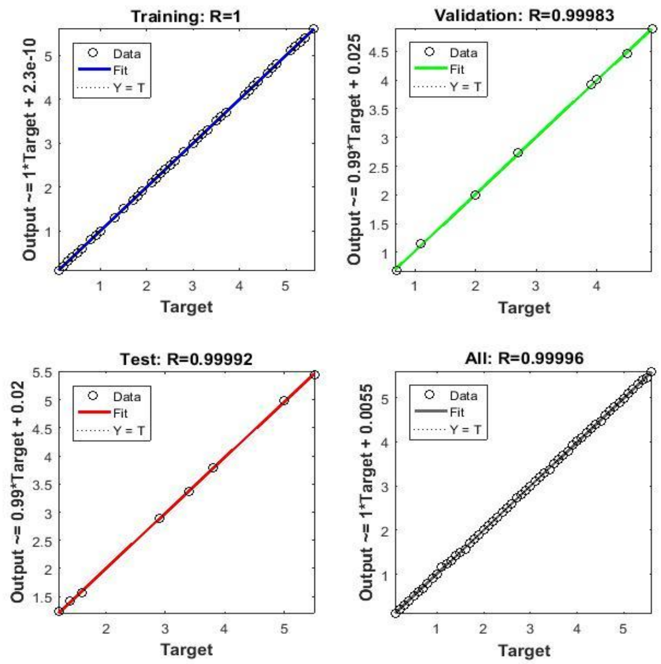

Figure 10.a.Predictor Regression of NNF for Iron shield with thickness= 4 cm.

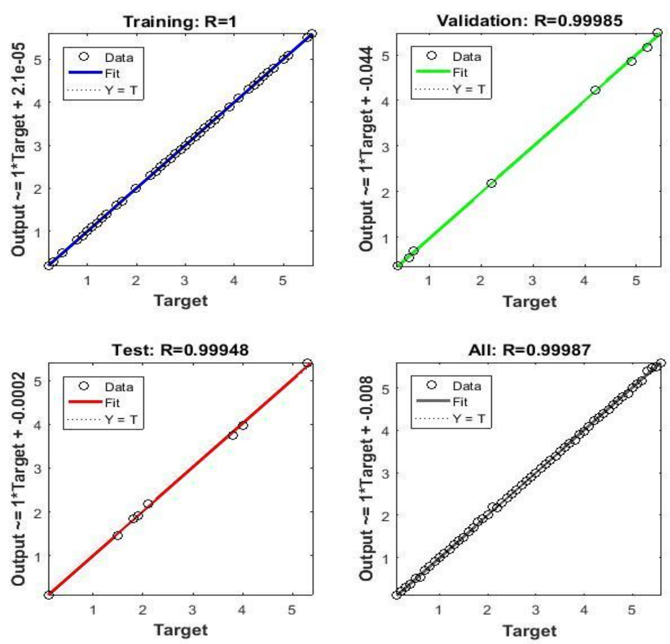

Figure 10.b. Predictor Regression of NNF for Tungsten shield with thickness= 4 cm.

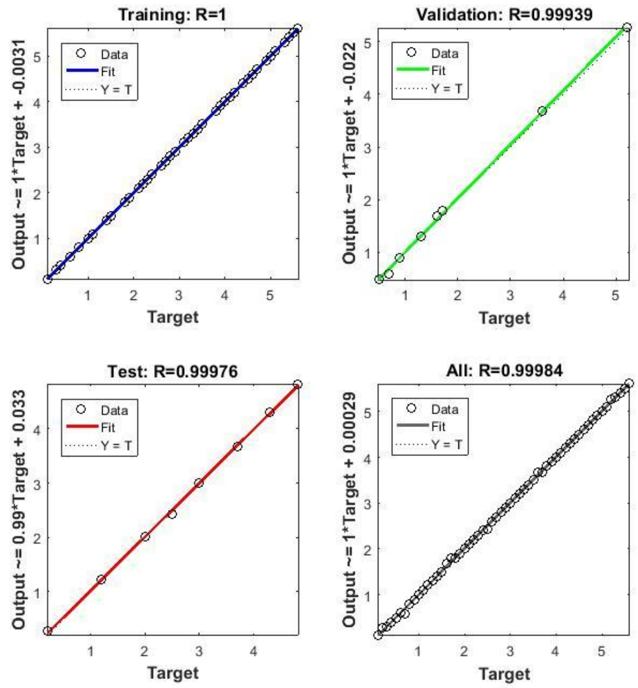

Figure 10.c. Predictor Regression of NNF for Tungsten alloy shield with thickness= 4 cm.

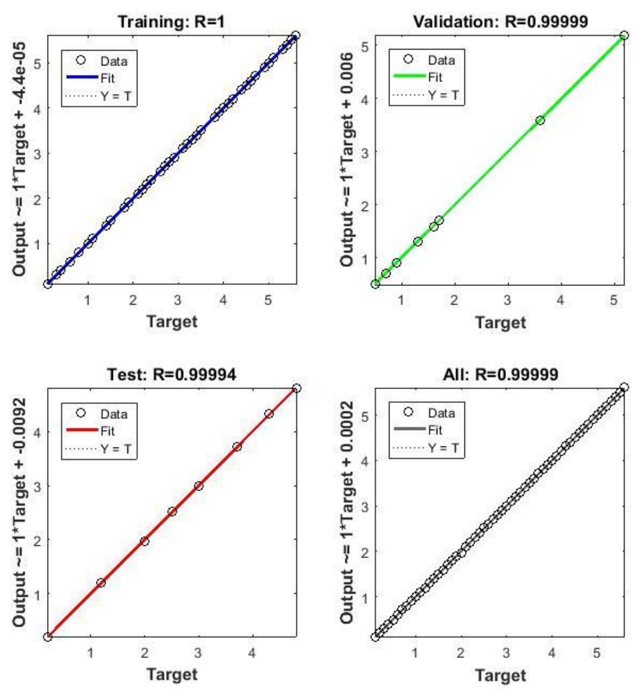

Figure 10.d. Predictor Regression of NNF for Iron shield with thickness= 5 cm.

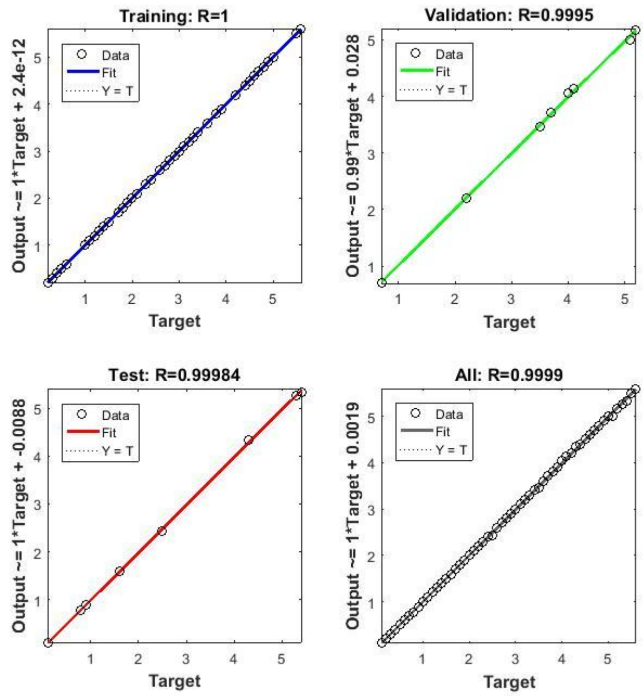

Figure 10.e. Predictor Regression of NNF for Tungsten shield with thickness= 5 cm.

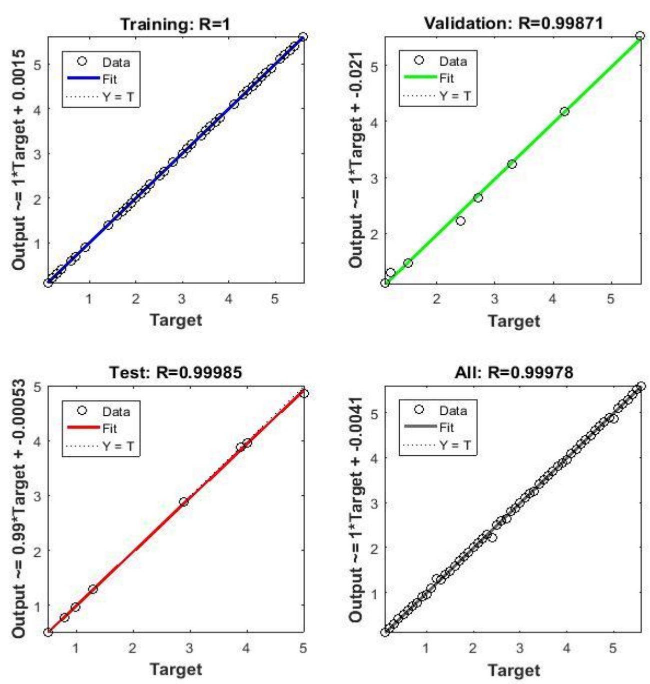

Figure 10.f. Predictor Regression of NNF for Tungsten alloy shield with thickness= 5 cm.

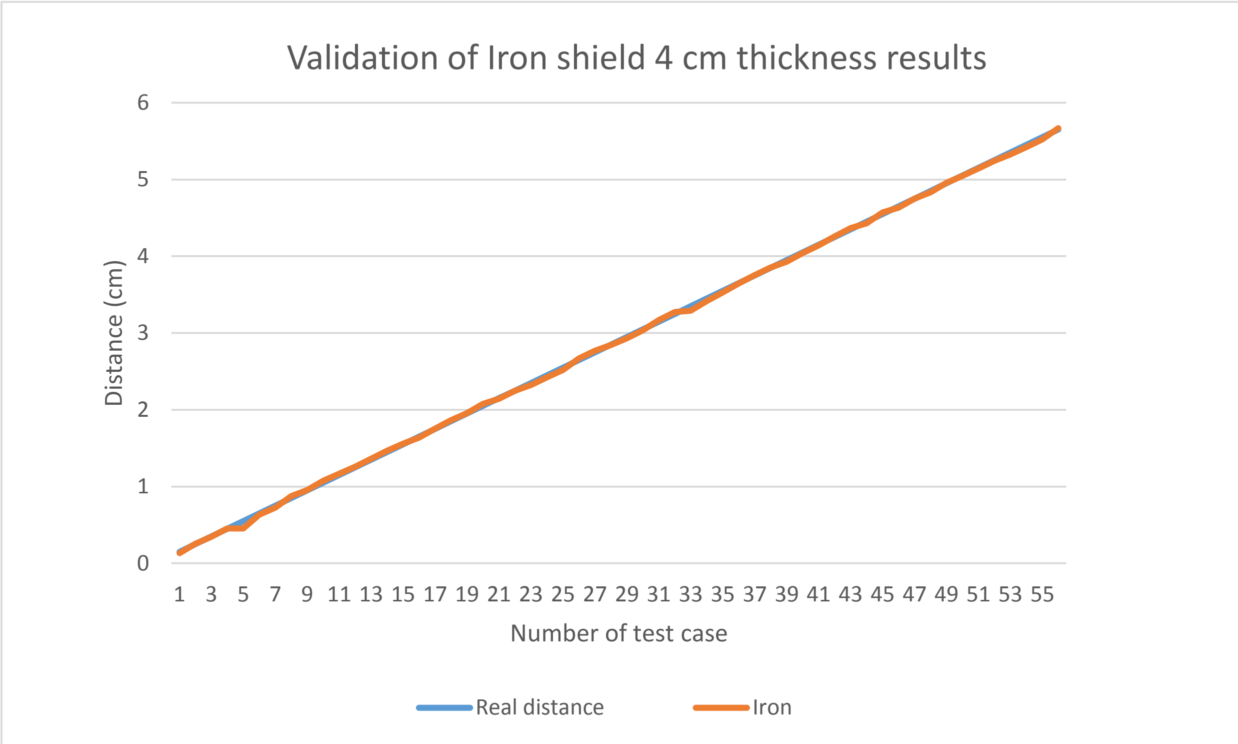

Figure 11.a. Validation of Neural net fitting algorithm on MCNP results based on 56 test cases for Iron shield with thickness = 4 cm.

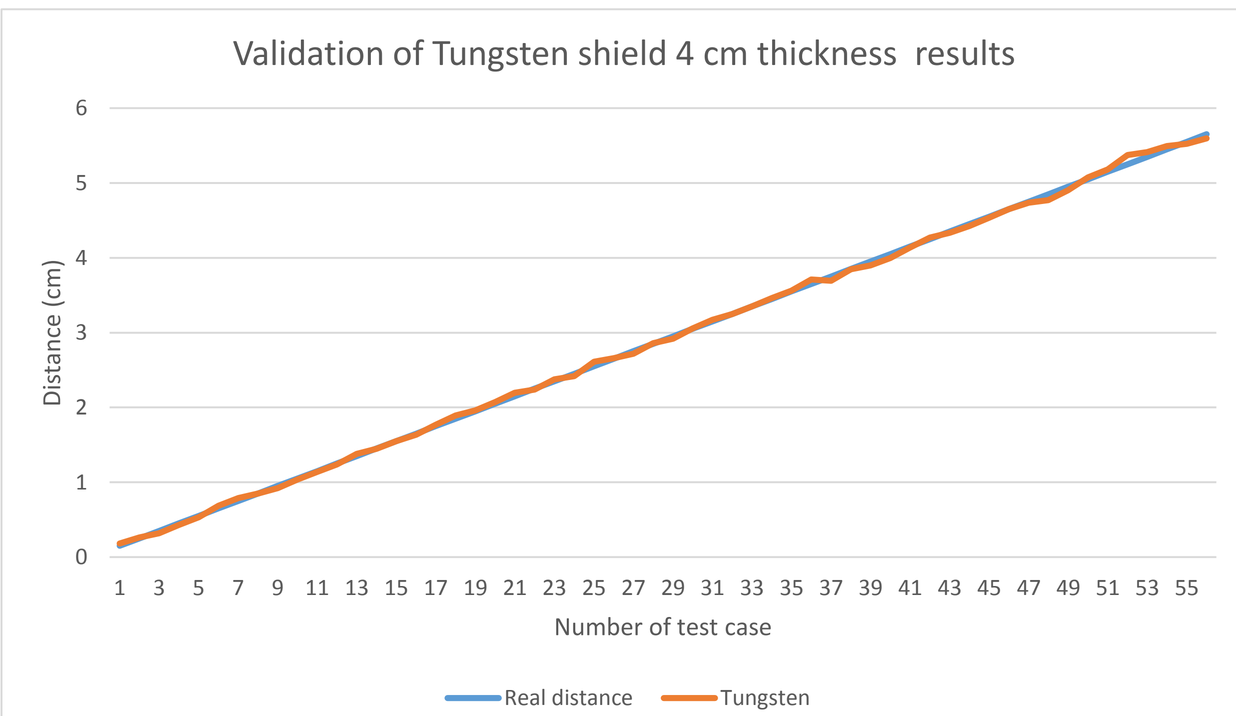

Figure 11.b. Validation of Neural net fitting algorithm on MCNP results based on 56 test cases for Tungsten shield with thickness = 4 cm.

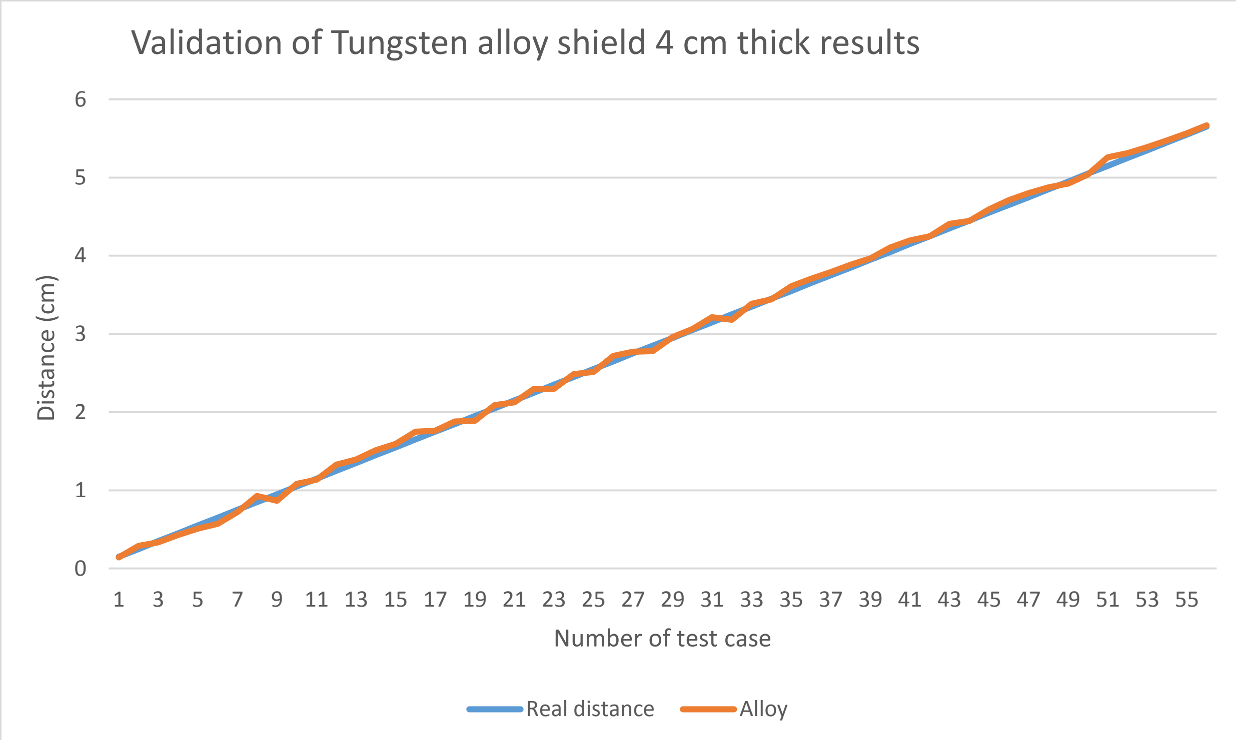

Figure 11.c. Validation of Neural net fitting algorithm on MCNP results based on 56 test cases for Tungsten alloy shield with thickness = 4 cm.

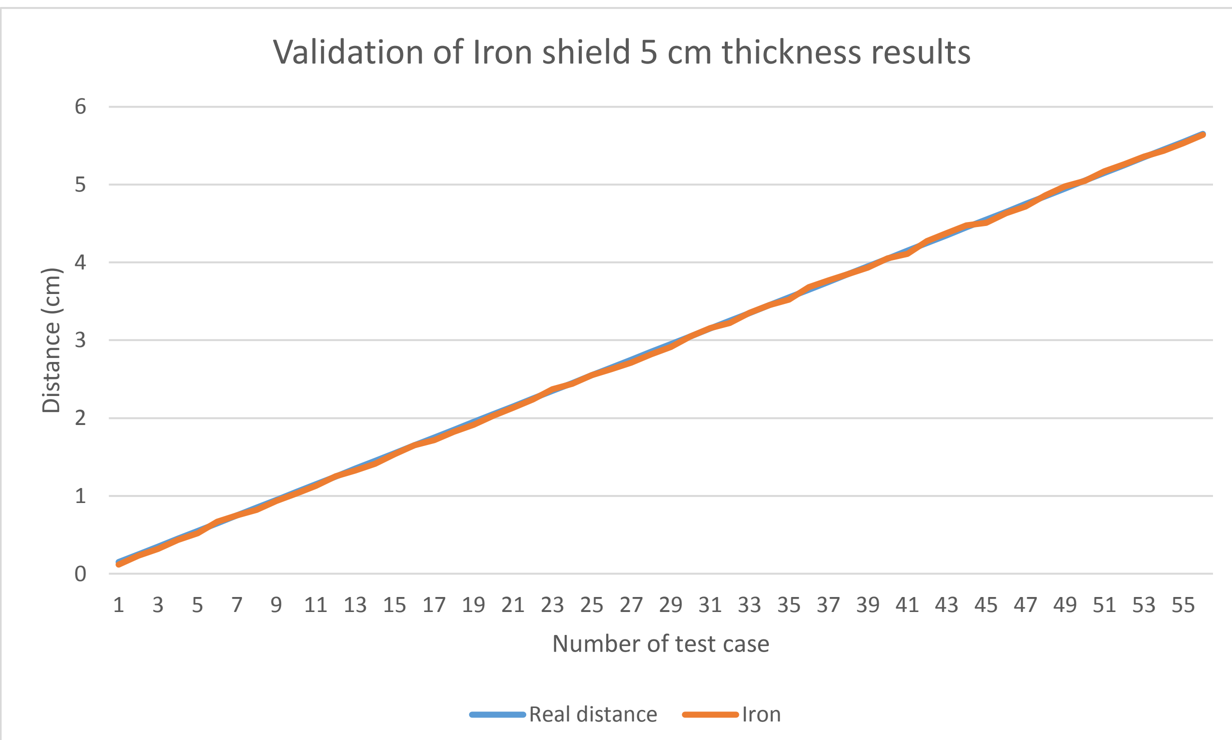

Figure 11.d. Validation of Neural net fitting algorithm on MCNP results based on 56 test cases for Iron shield with thickness = 5 cm.

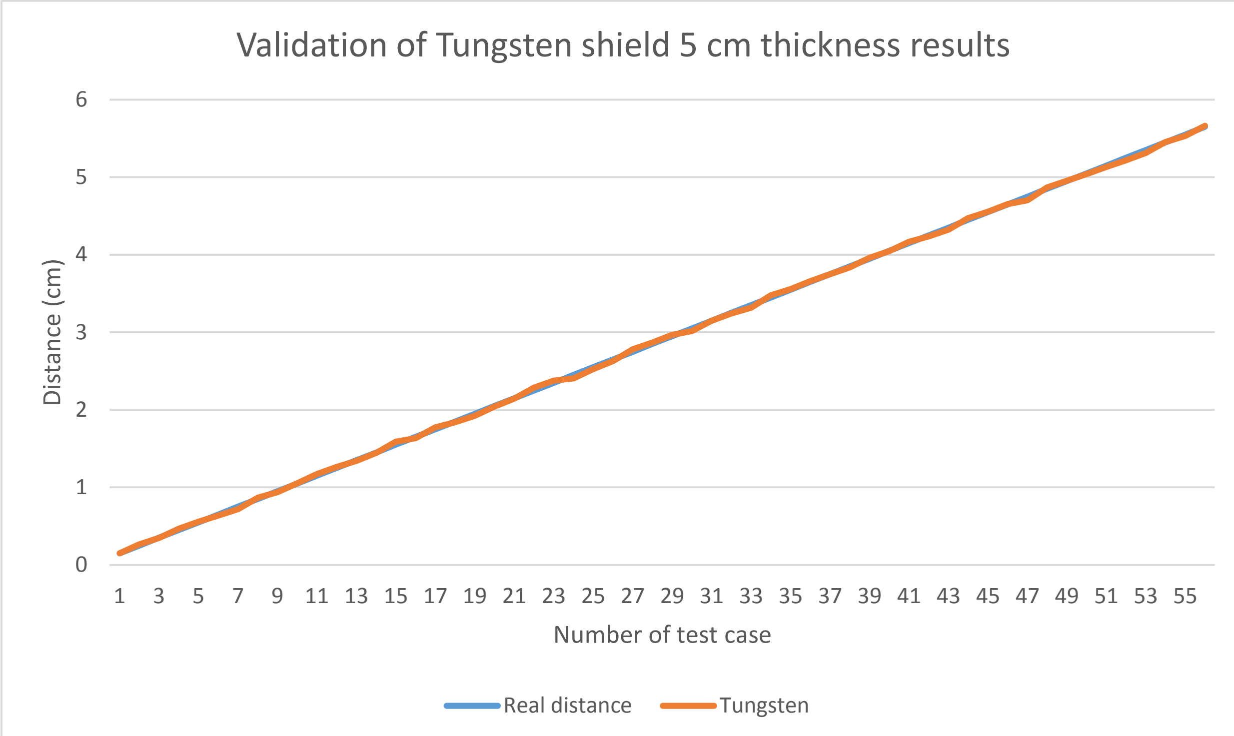

Figure 11.e. Validation of Neural net fitting algorithm on MCNP results based on 56 test cases for Tungsten shield with thickness = 5 cm.

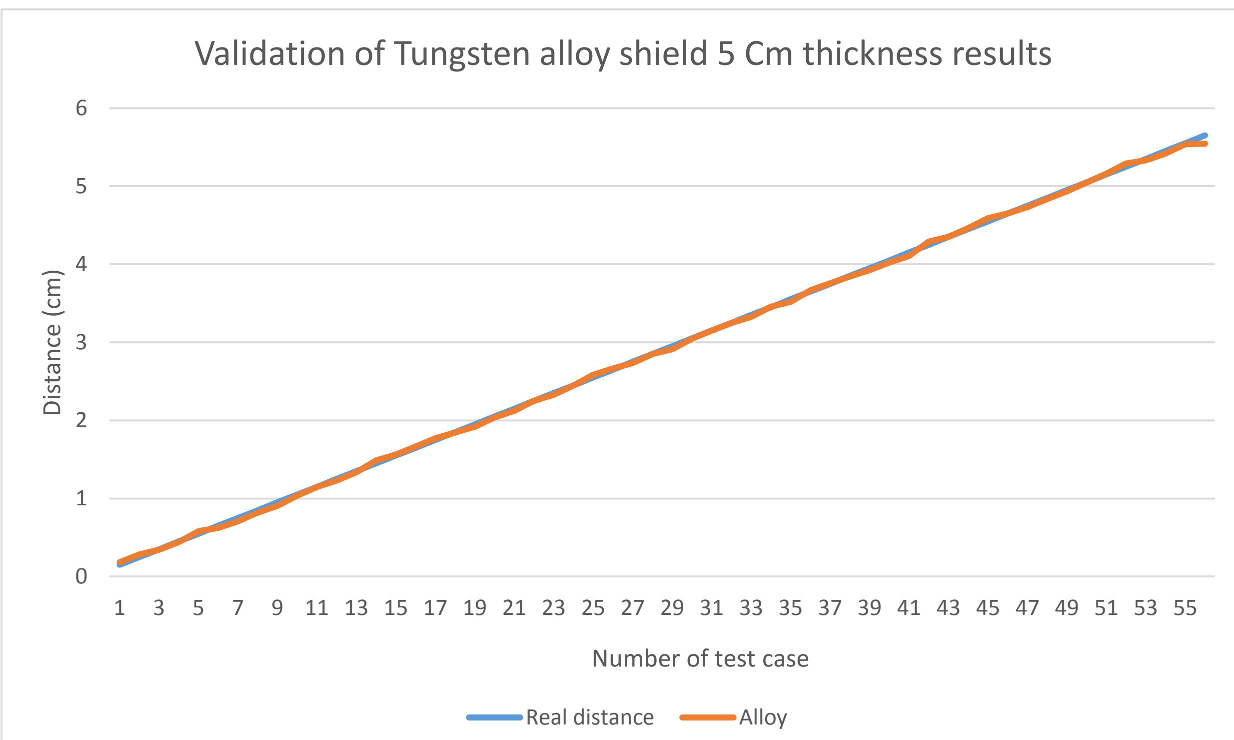

Figure 11.f. Validation of Neural net fitting algorithm on MCNP results based on 56 test cases for Tungsten alloy shield with thickness = 5 cm.

Table 3. Validation results of Neural net fitting NNF on MCNP results		
Material, thickness	MAE, cm	Standard error, cm
Iron, 4 cm	0.01685	0.002013
Tungsten, 4 cm	0.02738	0.003091
Tungsten alloy, 4 cm	0.04128	0.003352
Iron, 5 cm	0.01913	0.001574
Tungsten, 5 cm	0.01684	0.001621
Tungsten alloy, 5 cm	0.02026	0.002361

Neutrons Q-Value Calculations

The main reason for calculating the Q-value is to optimize the different collimator parameters in order to achieve the highest Q-value in order to protect the BGO detectors from the radiation damage that can be caused by the neutrons reaching the detector. The neutrons Q-value was calculated for all the proposed materials and the two proposed thicknesses of the collimator with variation in the distance of the first collimator plate from the center of the neutron beam for each BGO detector as shown in figures 12.a – 12.j.

Symmetry has been observed between the first five channels and the second five channels, due to the symmetry in their spatial distribution as shown in figures 3, and 4. In order to simplify the process of analyzing the results, the symmetry mentioned previously was used to compare between the different parameters for half the number of channels. It was observed that a five cm thick tungsten collimator gives the highest Q-value for four of the studied channels, and the highest Q-value is at these four channels existed at a distance of the first plate from the center of the neutron beam ranging from zero to 3 cm as shown in figure 13. It was also observed that at a distance ranging from zero to 3 cm the curves have almost identical behavior except that each channel has a higher curve than the previous one. Therefore the distance is chosen for the highest point in the lowest curve.

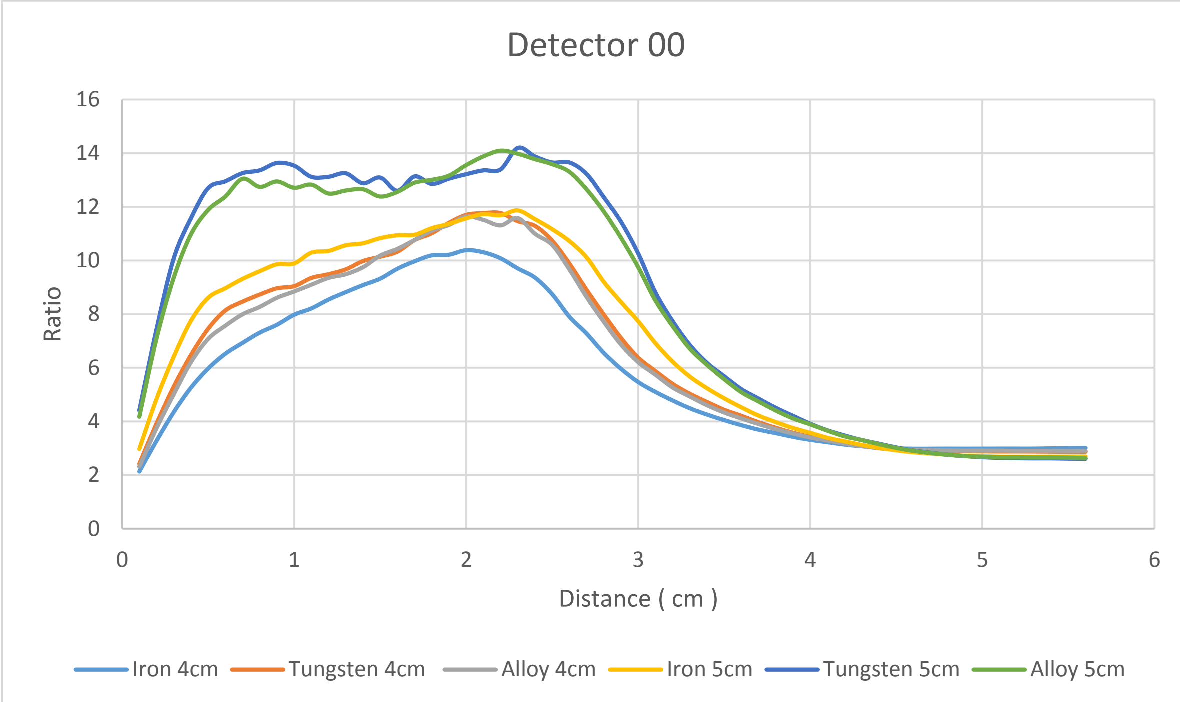

Figure 12.a. Neutrons Q value for detector 00.

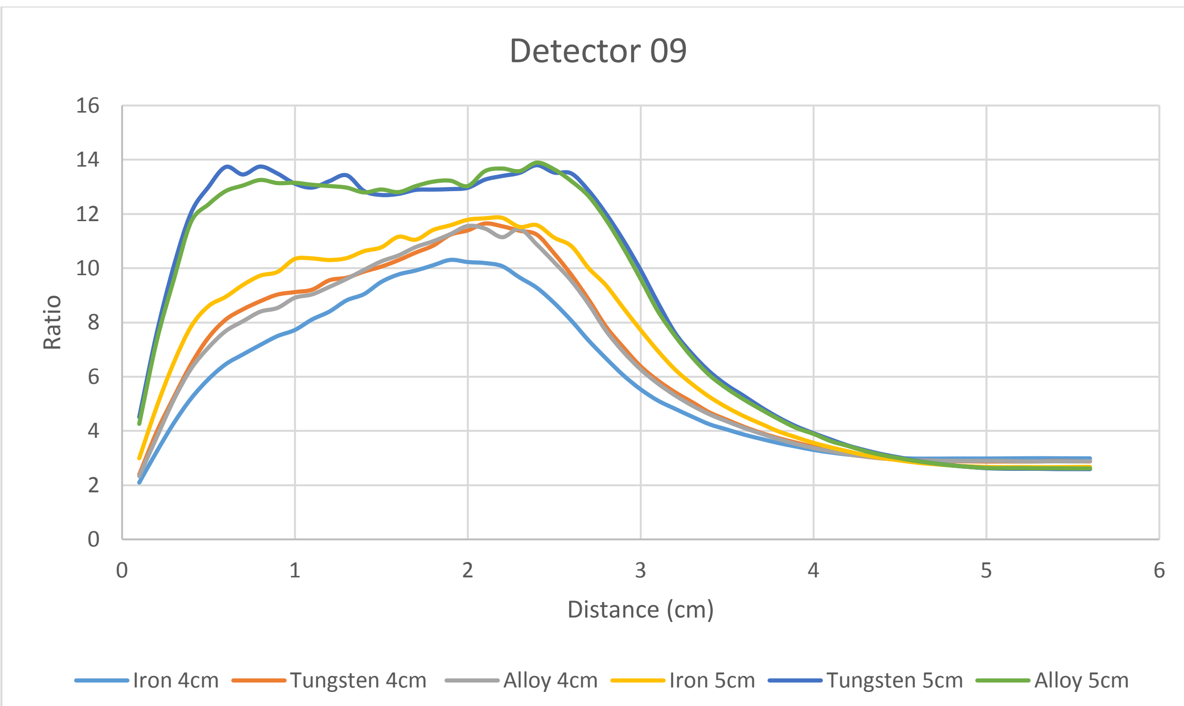

Figure 12.b. Neutrons Q value for detector 09.

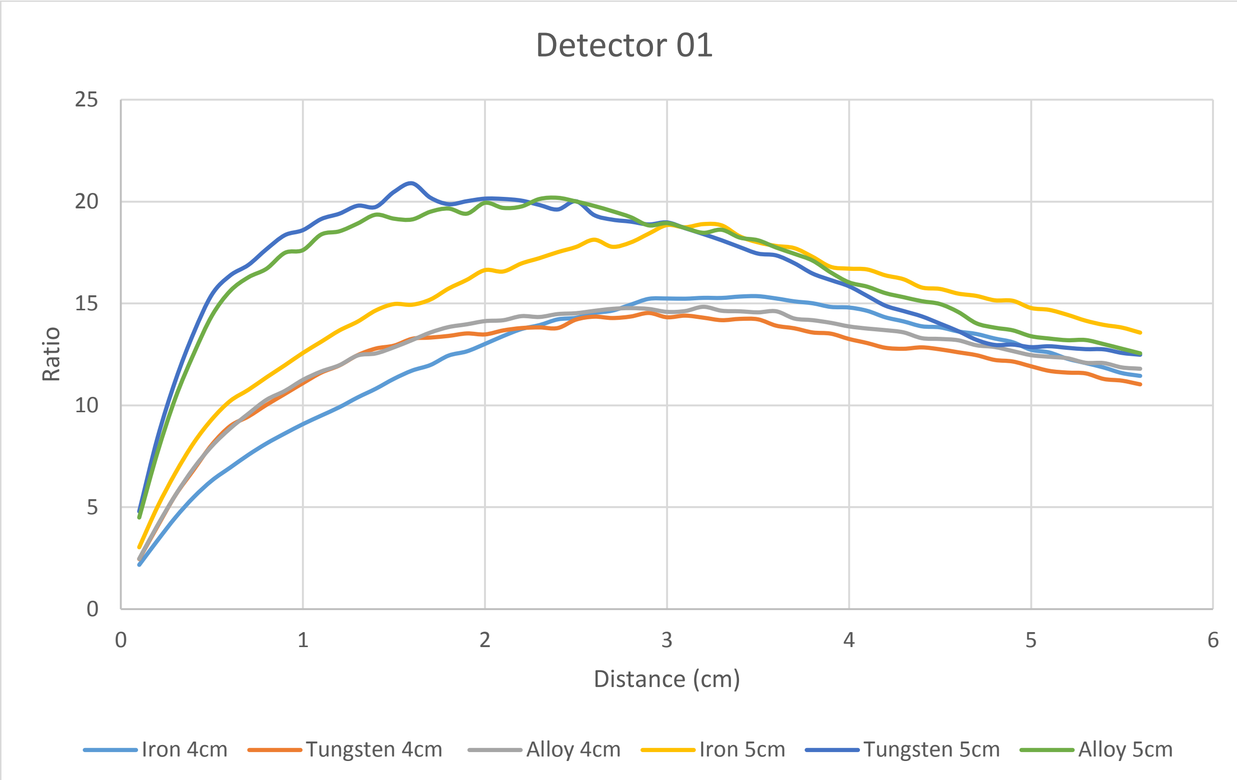

Figure 12.c. Neutrons Q value for detector 01.

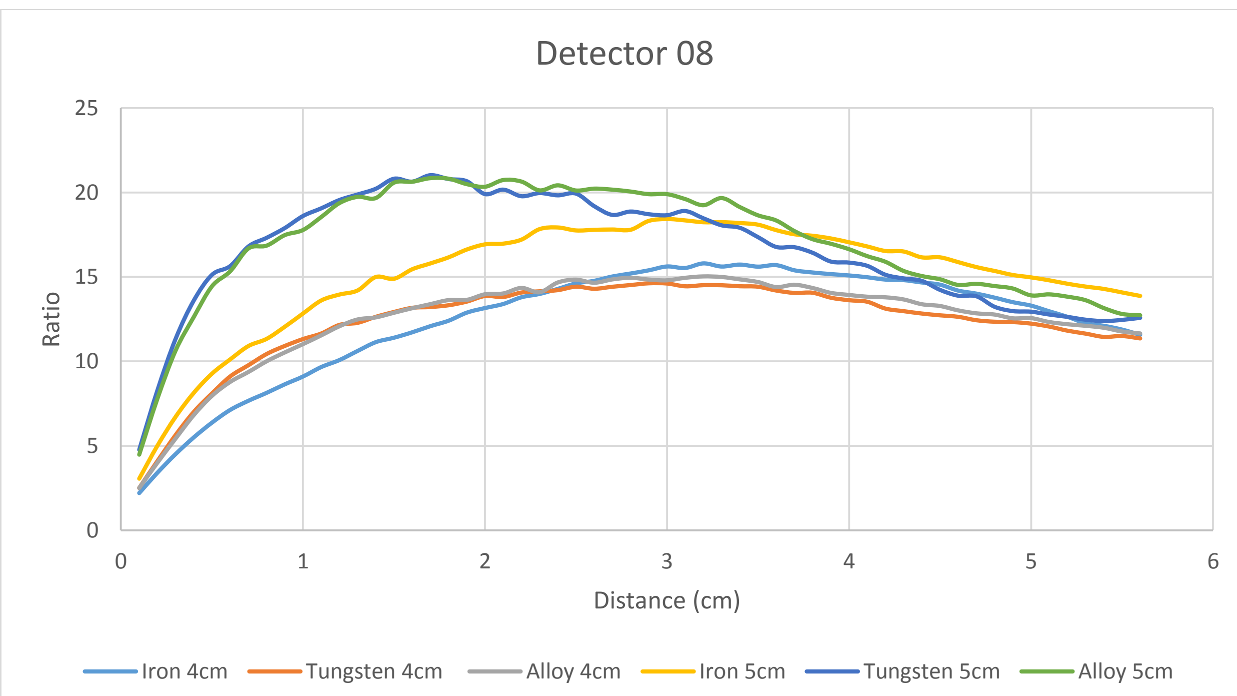

Figure 12.d. Neutrons Q value for detector 08.

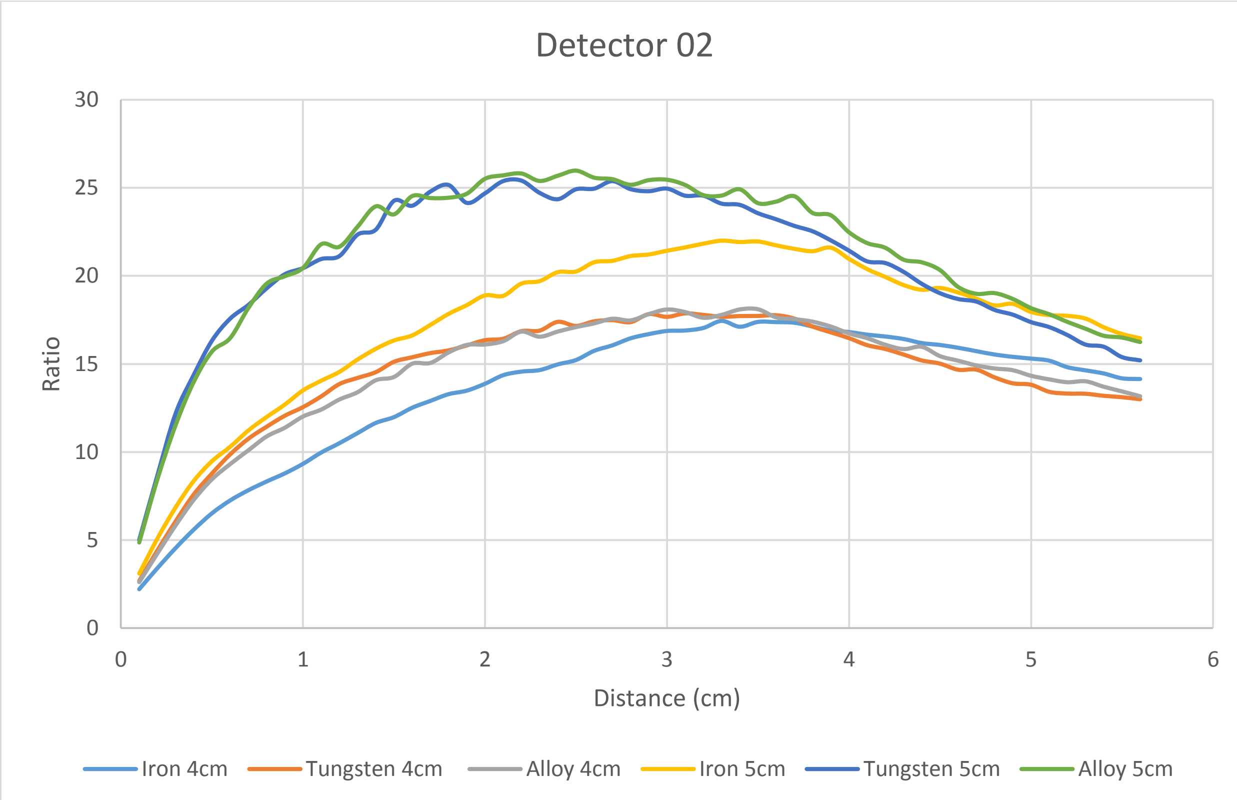

Figure 12.e. Neutrons Q value for detector 02.

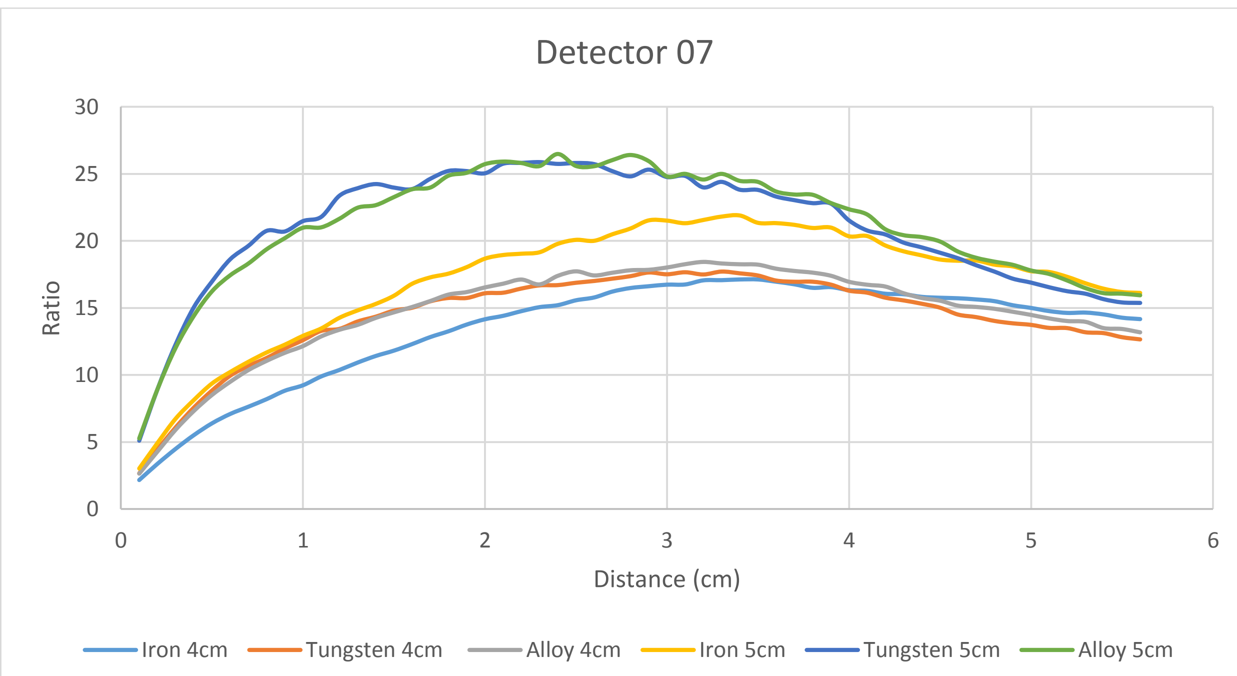

Figure 12.f. Neutrons Q value for detector 07.

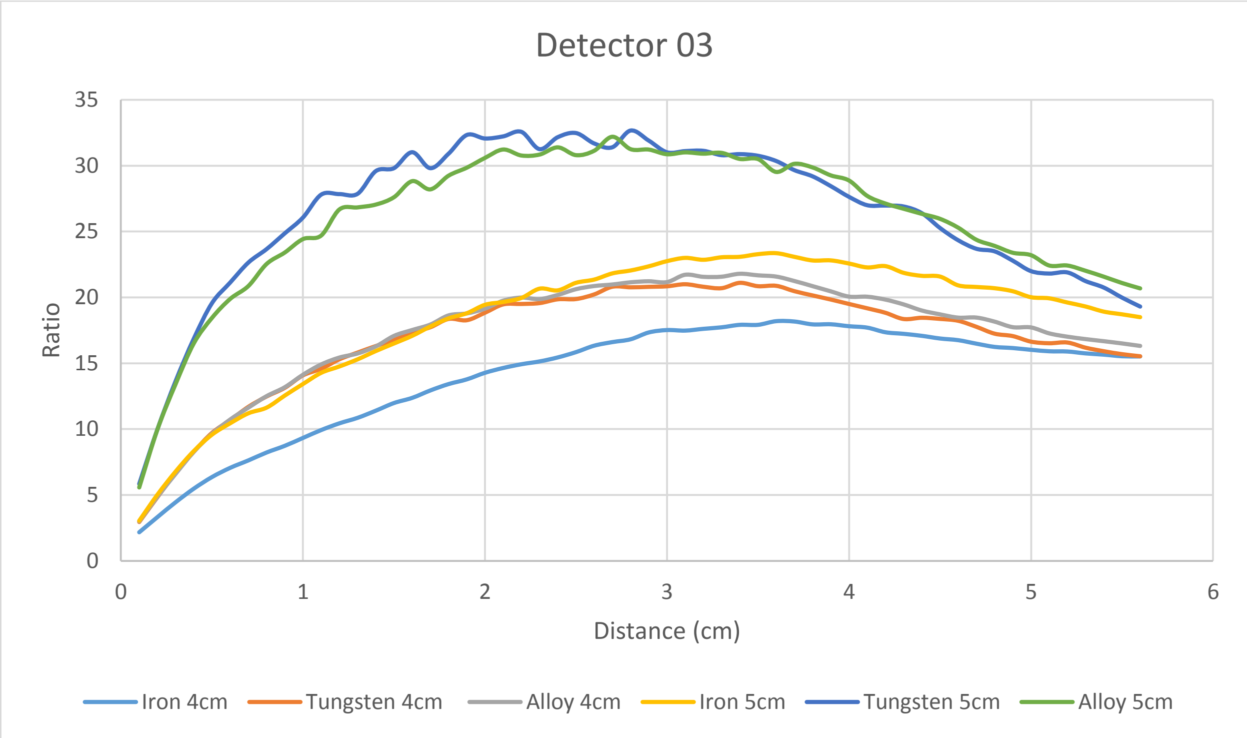

Figure 12.g. Neutrons Q value for detector 03.

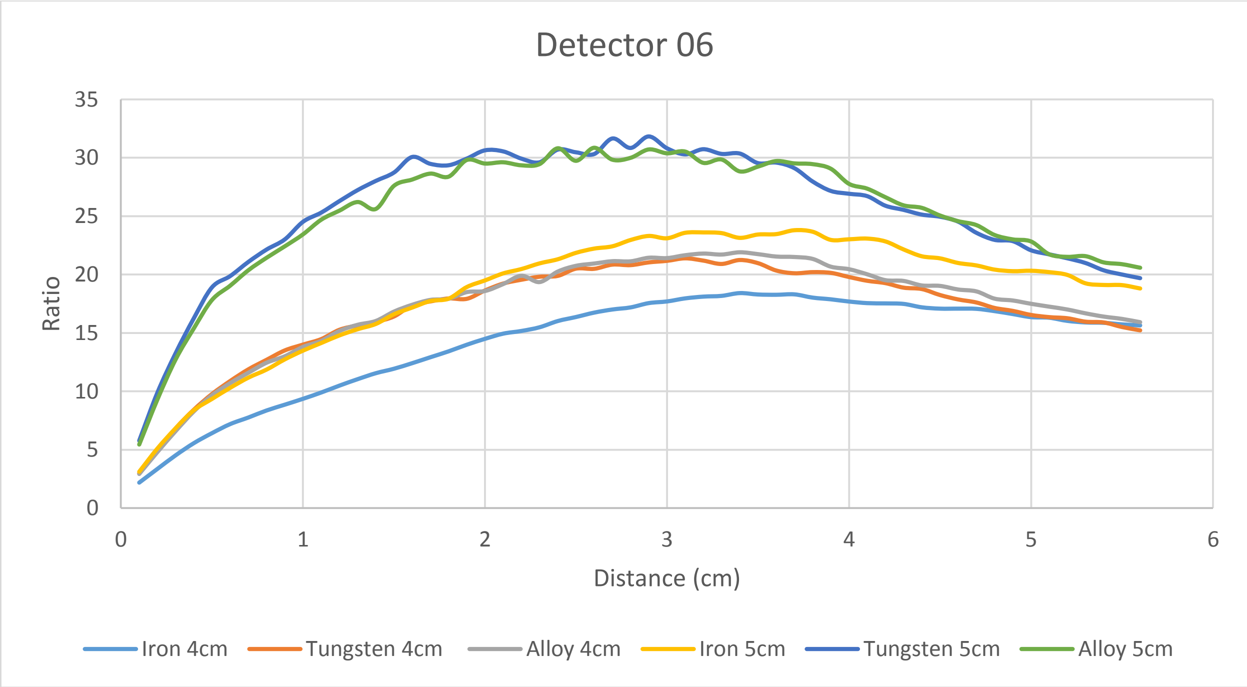

Figure 12.h. Neutrons Q value for detector 06.

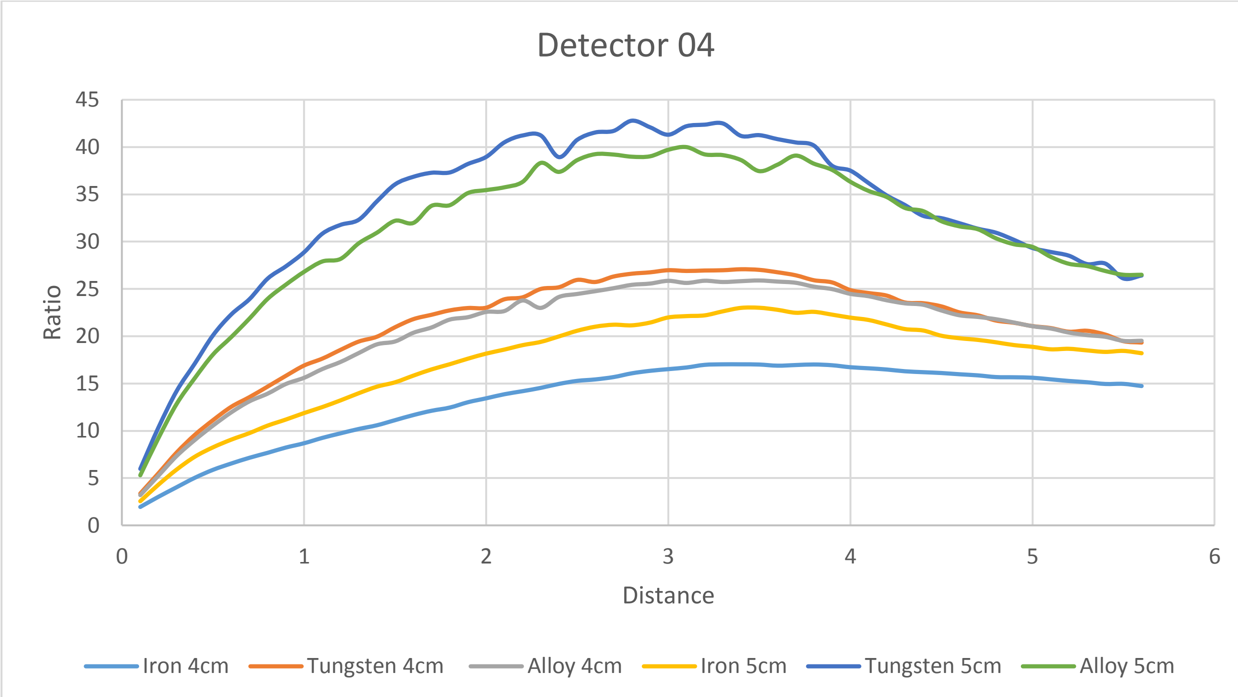

Figure 12.i. Neutrons Q value for detector 04.

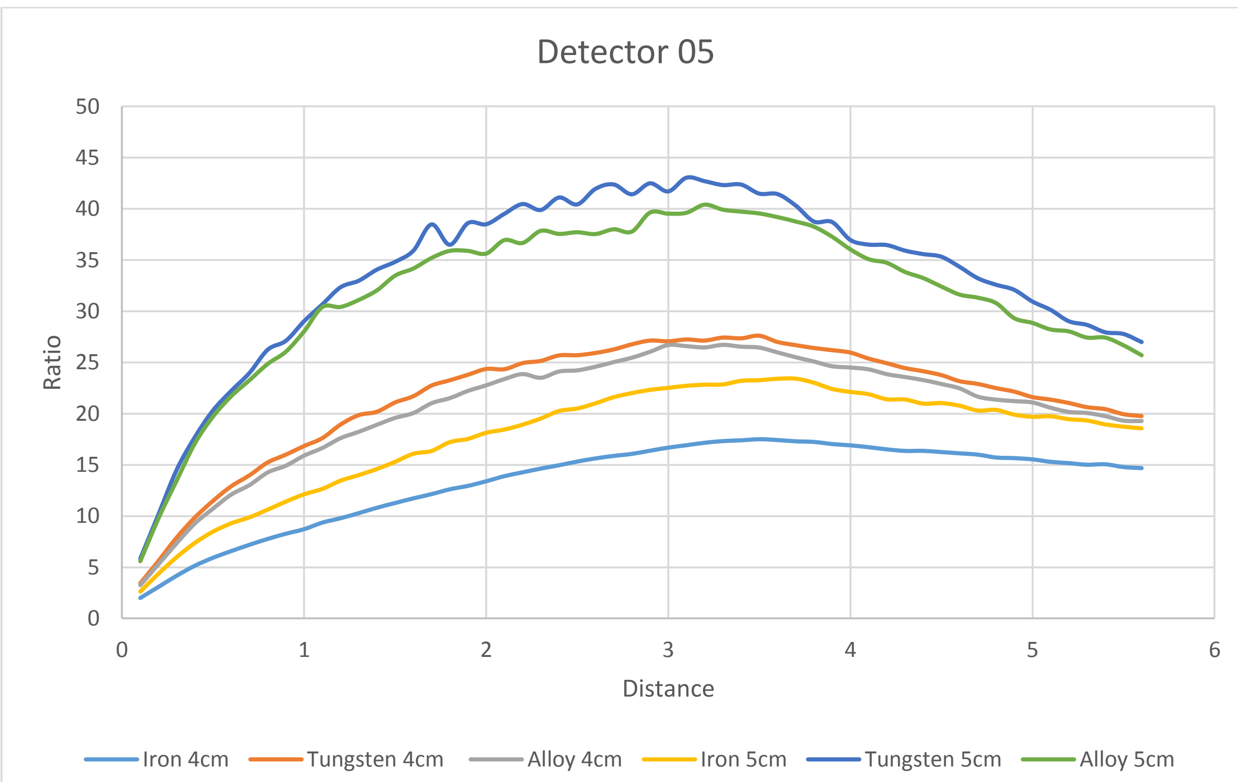

Figure 12.j. Neutrons Q value for detector 05.

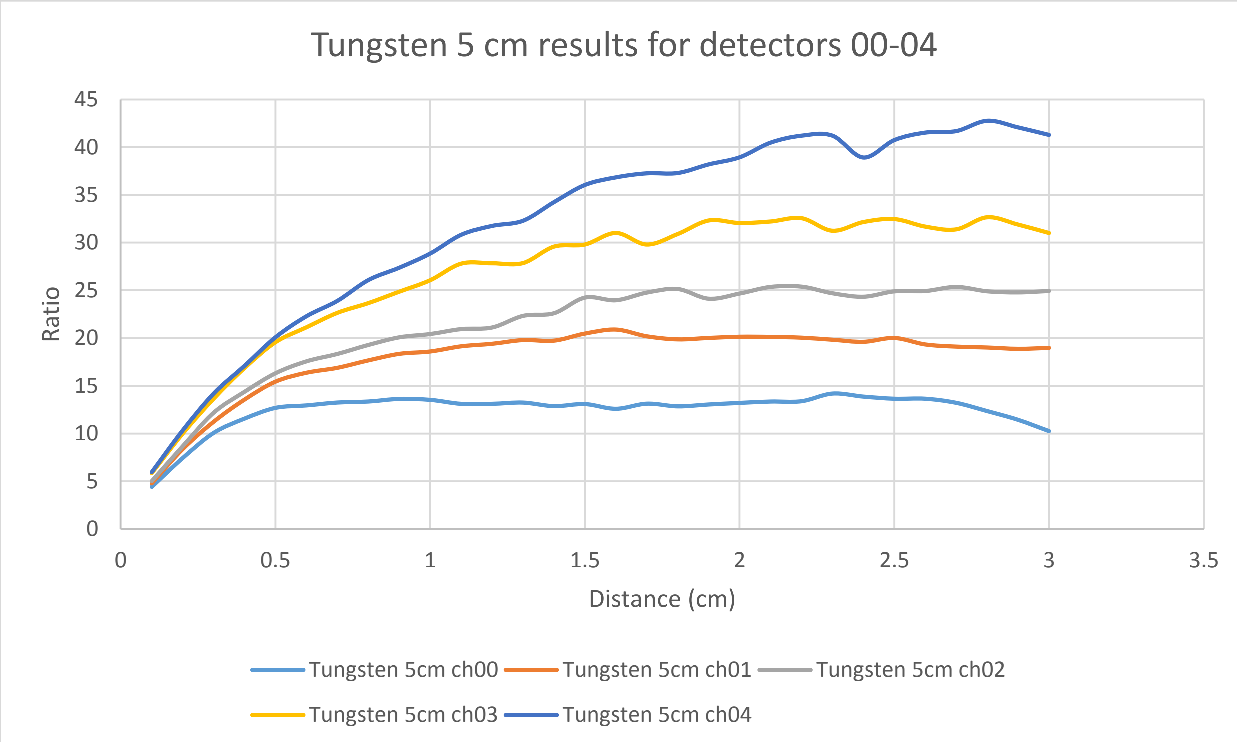

Figure 13. Tungsten 5 cm results for detectors 00-04.

Gamma Q-Value Calculations

Like the neutrons Q-value, the gamma Q-value was calculated for all the channels but for a different reason which is to minimize the gamma rays emitting from the inelastic scattering and radiative capture of the collimator material to the neutrons in order to minimize the background radiation reaching the detectors in order to prevent the overlapping of the collimator gamma peaks with the sample peaks in order to facilitate the process of the neutron spectroscopy. Figures 14.a – 14.j show the different variations of the different shielding-collimator parameters for each channel.

The behavior of Iron shield of 4 or 5 cm is almost stable with the distance but the behavior of Tungsten shield and Tungsten alloy shield (90% Tungsten) was observed to be unstable, instability of the behavior of tungsten and tungsten alloy shields refers to the statistical errors in the simulation, but the physical dependence of the ratio on the distance is not affected.

As in neutron Q-value, it was observed that the highest of the Q-values are achieved when the collimator is Tungsten and its sheets are of 5 cm thick, and the operating distance ranges from 0 to 3 cm. Therefore, the operating distance will be chosen based on the highest Q-value for the lowest channel curve, which was found to be 0.5 cm as shown in figure 15. Since the 0.5 cm distance is not practical, therefore another distance was chosen based on the same methodology which was found to be 1 cm.

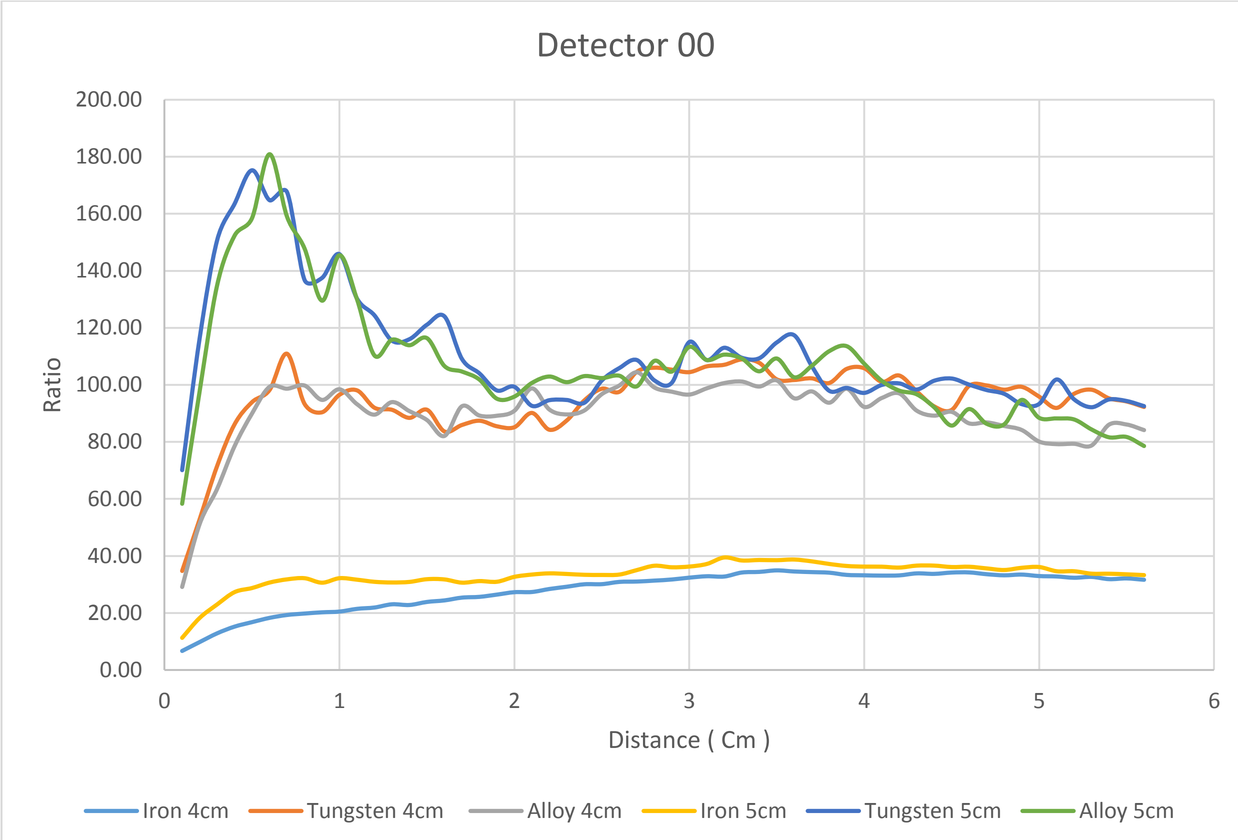

Figure 14.a. Gamma Q value for detector 00.

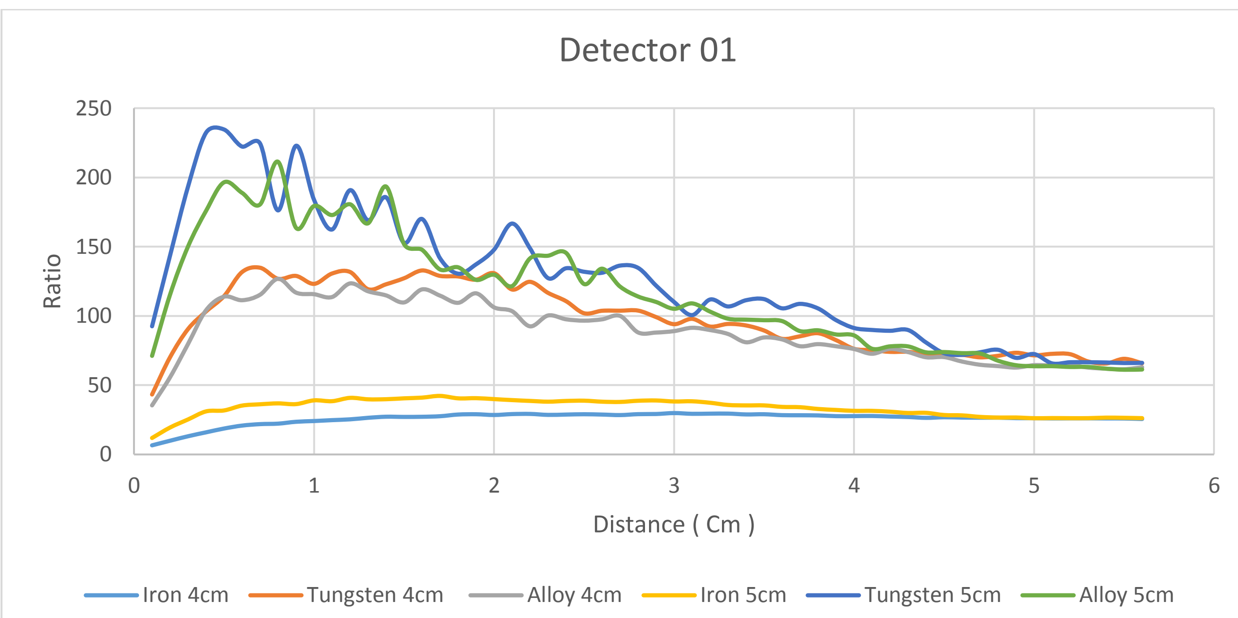

Figure 14.b. Gamma Q value for detector 01.

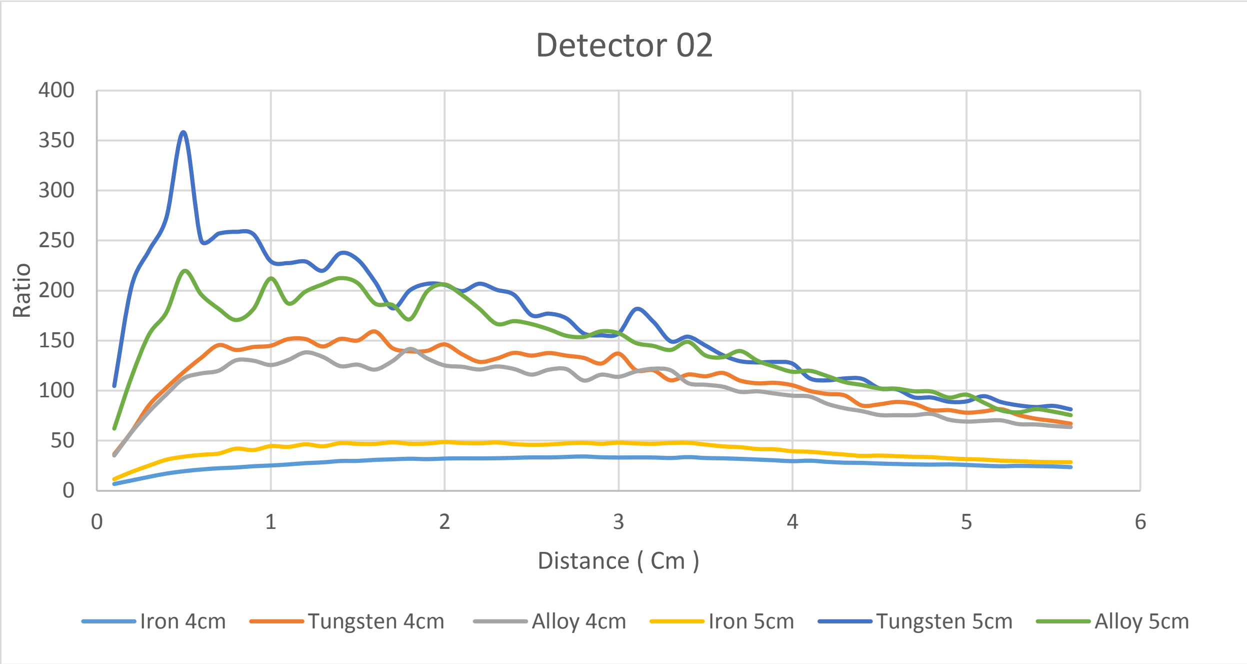

Figure 14.c. Gamma Q value for detector 02.

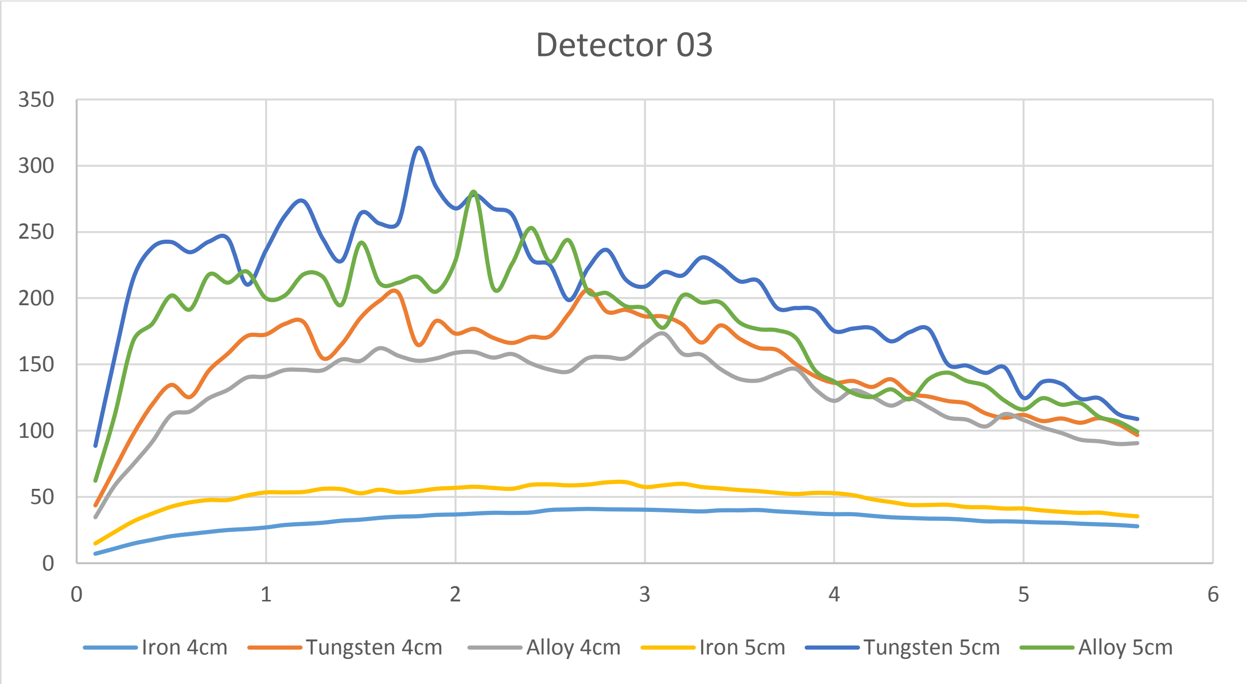

Figure 14.d. Gamma Q value for detector 03.

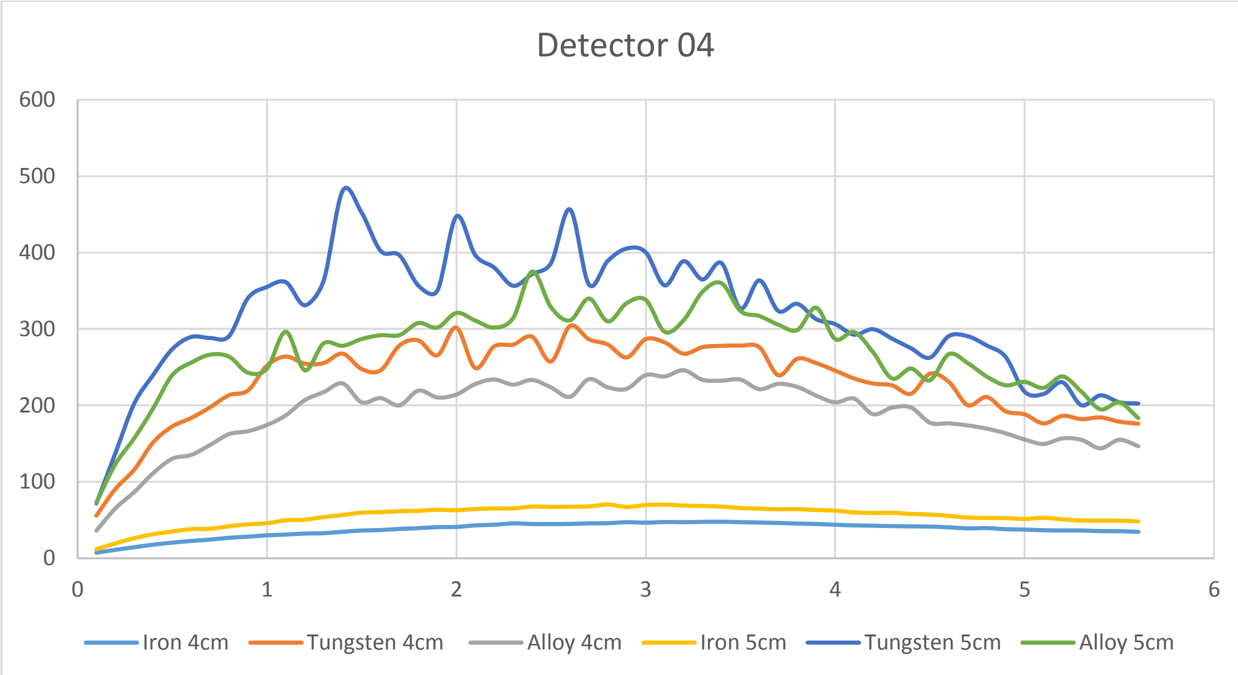

Figure 14.e. Gamma Q value for detector 04.

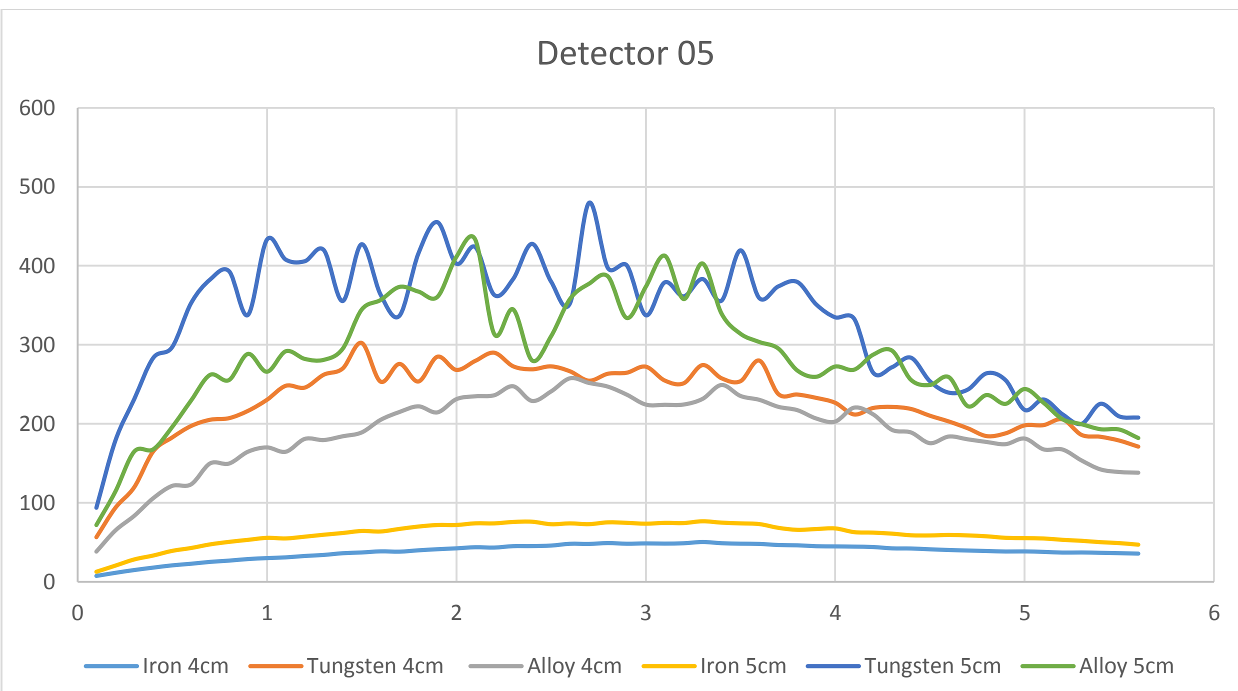

Figure 14.f. Gamma Q value for detector 05.

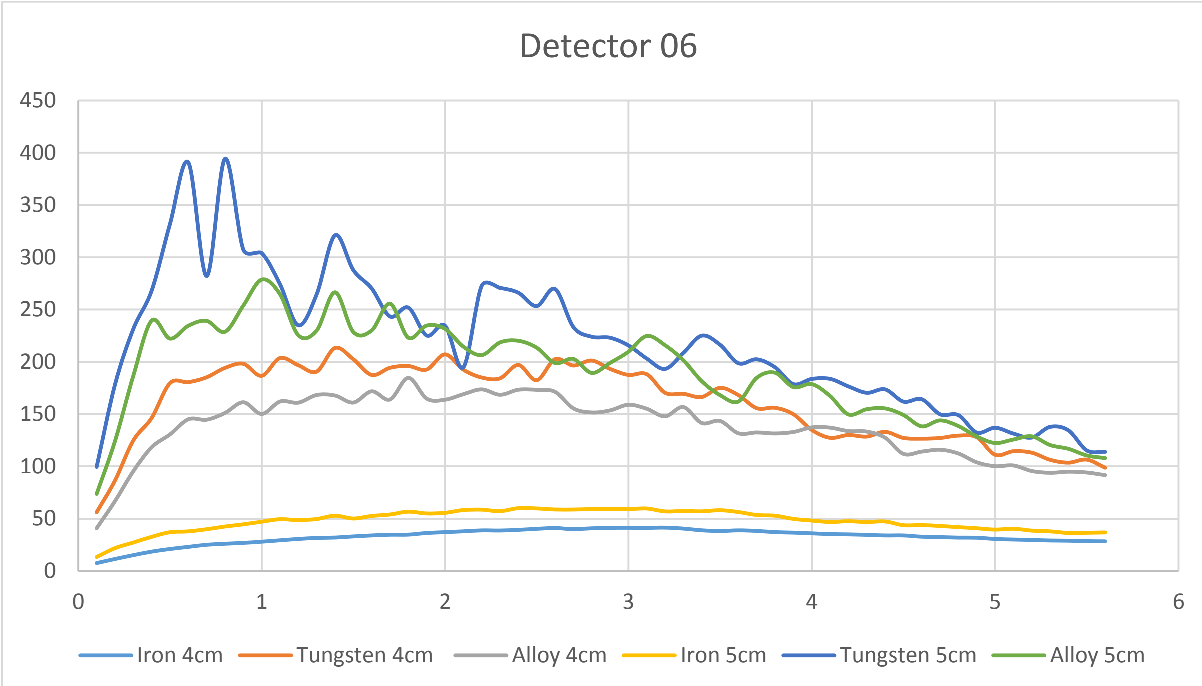

Figure 14.g. Gamma Q value for detector 06.

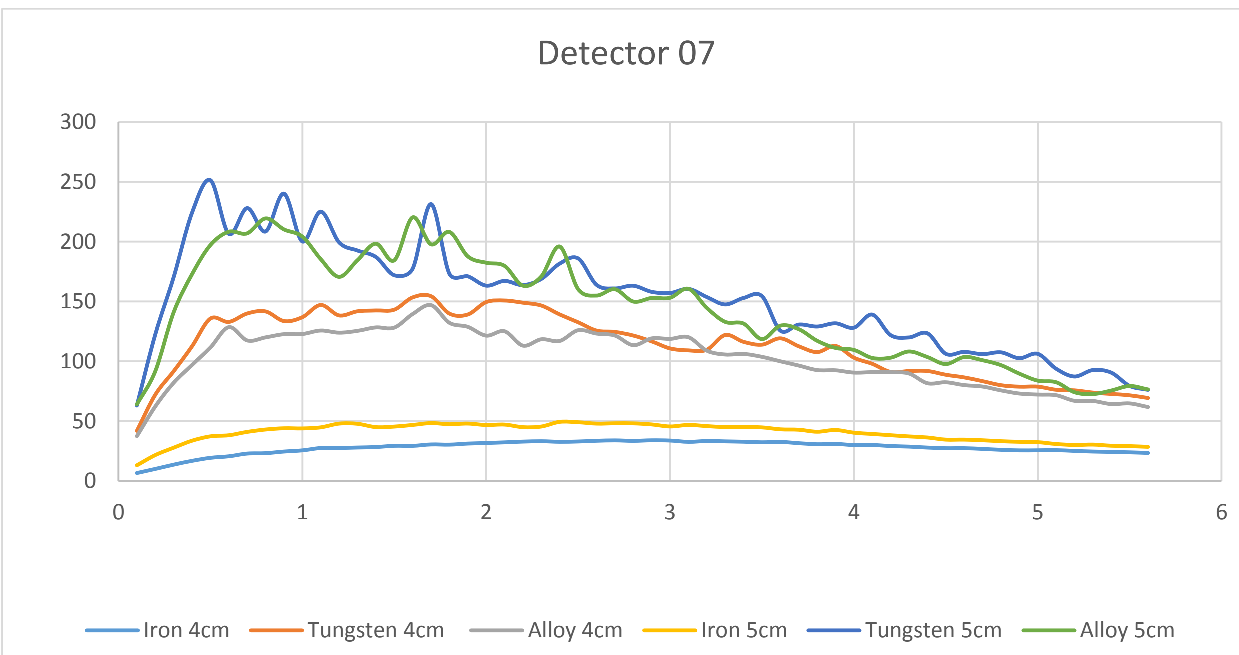

Figure 14.h. Gamma Q value for detector 07.

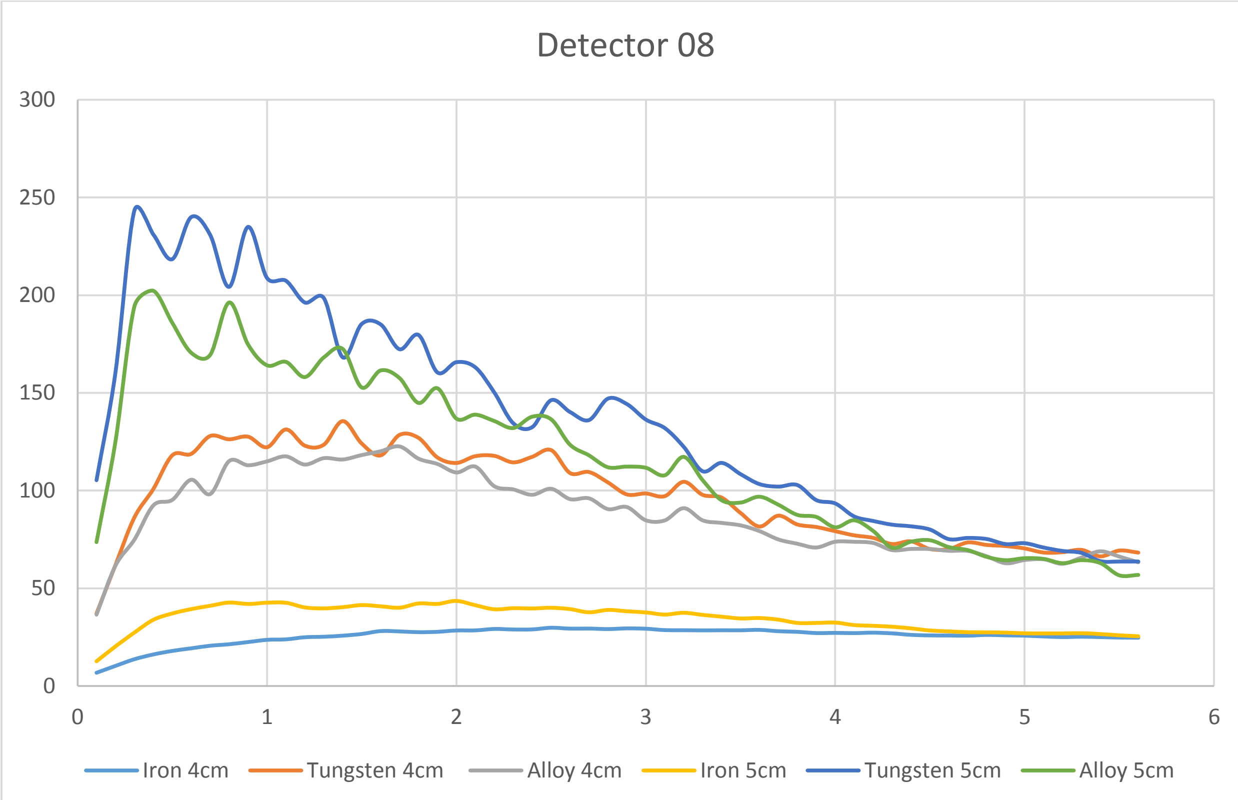

Figure 14.i. Gamma Q value for detector 08.

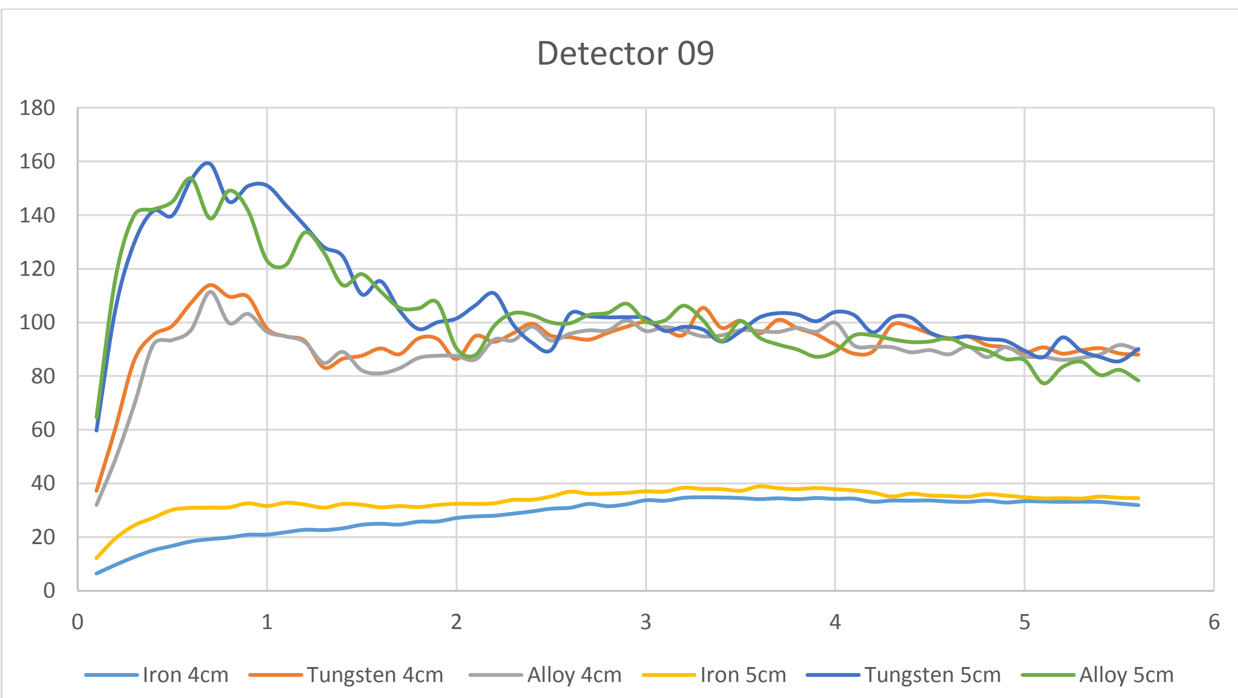

Figure 14.j. Gamma Q value for detector 09.

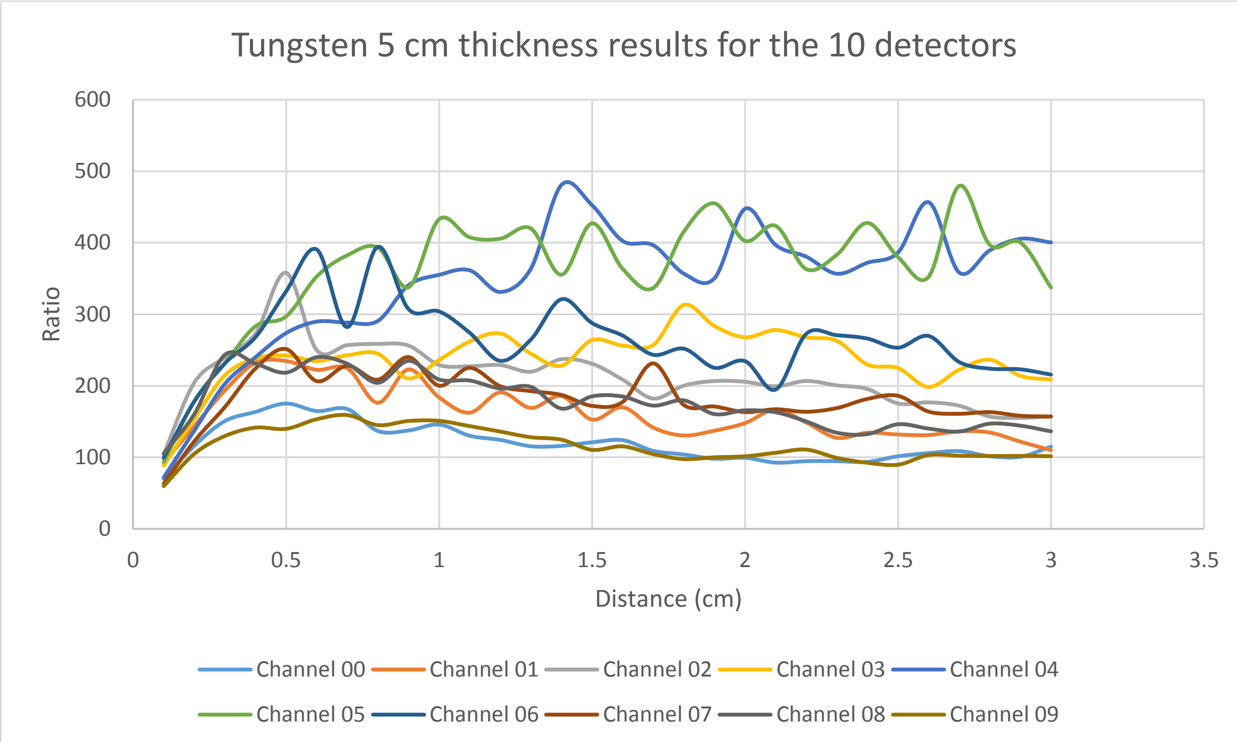

Figure 15. Tungsten 5 cm thickness for the 10 BGO detectors.

Conclusion and Future Work

From the above discussion, it was proven that the neural networks can be used for solving the neutron collimator parameters optimization problem based on the desired value for saving time and computational power instead of the design iterations approach.

Considering the ROMASHA setup, the optimum collimator parameters for the neutron Q-value was if the shielding- collimator assembly was made of Tungsten of 5 cm thickness for each plate, and a distance of 2.3 cm. while in case of gamma Q-value, the distance was concluded to be of 1 cm.

Future Work can include the generalization of this approach for all the proposed collimator materials and geometries.

Acknowledgment

Concluding my report I would like to express my gratitude to the whole staff members of TANGRA setup project and special thanks to my scientific supervisor Dr. Vadim Skoy and Mr. D.N. Grozdanov for their invaluable assistance in performing of this work.

I'm also grateful to JINR University Centre, especially Ms. Elena Karpova for providing me such an opportunity to work in one of the JINR's laboratories and immensely grateful to Frank Laboratory of Neutron Physics for the financial support of my summer program.

Special thanks to Dr. Dorota Chudoba and Ms. Julia Rybachuk for their help and care during my stay in Dubna.

Finally I would like to express my sincere gratitude to my mentor in Egypt Mr. Karim Hossny for helping me to get such an opportunity and his continuous support.

References

[1] "Neutron Generators for Analytical Purposes," IAEA, Vienna, 2012.

[2] Gurny, Kevin. An introduction to neural networks. England, University of Sheffield, 2004.

[3] Jolliffe, I. T., *Principal Component Analysis*, 2nd edition, Springer, 2002.

[4] E. S. Konobeevsky, L. N. Latysheva, N. M. Sobolevsky, and R. D. Ili," Optimizing the Collimator/Shielding Configuration of the NG-430 Neutron Generator", *Bulletin of the Russian Academy of Sciences. Physics, 2011, Vol. 75, No. 4, pp. 449–453, 2011.*

[5] D.L. Chichester and B.W. Blackburn, "Radiation fields from neutron generators shielded with different materials", Nuclear Instruments and Methods in Physics Research B 261 (2007) 845–849.

[6] K. Bergaoui, N. Reguigui , C. K. Gary , M. . A. Piestrup and J. T. Cremer, "Design, testing and optimization of a neutron radiography system based on a Deuterium–Deuterium (D–D) neutron generator," *Journal of Radioanalytical and Nuclear Chemistry,* 2013.

[7] I.N. Ruskov, Yu.N. Kopatch, V.M. Bystritsky *et al.,* TANGRA-Setup for the Investigation of Nuclear Fission induced by 14.1 MeV neutrons. Physics Procedia, 64 (2015) 163-170.

[8] Skoy, V.R., Kopatch Yu.N., Ruskov I., A versatile multi-detector gamma-ray spectrometry system for investigation of neutron induced reactions. 21st International Seminar on Interaction of Neutrons with Nuclei, ISINN-21, 20-25 May 2013, Alushta, Ukraine, pp. 242-248.

[9] D.N. Grozdanov, A.O. Zontikov, Optimization of" Romashka" setup for investigation of (*n, n0γ*)-reactions with tagged neutrons method, ISINN-23 proceedings: http:isinn.jinr.rupast-isinnsisinn-23program.html.

[10] Neutron generators for analysis of substances and materials. ING-27 gas-filled neutron tube based neutron generator of VNIIA, http://www.vniia.ru/eng/ng/docs/ing element eng.pdf.